Title
Integrated Maneuvering Control Design And Experiments: Report For Phase III

Authors
Hedrick, J. K.
Yoshioka, T.
Chen, Y. H.
et al.

Publication Date
1997

CALIFORNIA PATH PROGRAM
INSTITUTE OF TRANSPORTATION STUDIES
UNIVERSITY OF CALIFORNIA, BERKELEY

Integrated Maneuvering Control Design and Experiments: Report for Phase III

J.K. Hedrick, T. Yoshioka, Y.H. Chen, T. Connolly, L.R. Shen
University of California, Berkeley

California PATH Research Report
UCB-ITS-PRR-97-30

This work was performed as part of the California PATH Program of the University of California, in cooperation with the State of California Business, Transportation, and Housing Agency, Department of Transportation; and the United States Department of Transportation, Federal Highway Administration.

July 1997

ISSN 1055-1425

REPORT FOR PHASE-III

Integrated Maneuvering Control Design and Experiments (M.O.U.#99)

Submitted By:

J.K.Hedrick (P.I.)
T.Yoshioka
Y.H.Chen
T.Connolly
L.R.Shen

University of California ,Berkeley
1996

Abstract

In this report, a control system called CICC has be presented for vehicle-followig and collision-avoidance. This system contains several sub-systems, such as cruise control and distancing control, each of which has also been described. While each sub-system is designed to maintain the system stability, CICC achieves good comfort as well as sufficient capacity of avoiding collisions.

The performances of a CICC have been evaluated through simulations with a non-linear vehicle model . The vehicle model used in this report is the same as that presented in [9], which has been used for the simulations in the PATH project. This vehicle model contains several non-linearities to emulate real vehicle responses while eliminating excessive complexity. **A** simplified vehicle model to implement CICC has also been presented. When implementing a CICC, the robustness of CICC should be evaluated because there must exist some modeling errors. The simulation consist of various scenarios on highways, such as catching-up and cutting-in,and,depending on these situations, the performance of a CICC will be compared with nominal headway control and with other CICC's, whose specific functions are turned off.

Vehicles within a platoon depend on a communication network to provide the information necessary to maintain stable control at such close intervehicular spacings. To join two platoons together, or to split one platoon apart "on the fly" requires that this communication network be disturbed. **A** protocol must be developed for each of these maneuvers such that the control information being passed through this network remains as unperturbed as possible during the reconfiguration of the platoon networking structure.

A protocol for a platoon split maneuver has been developed in chapter 3, and is being readied for testing. It was designed with a multilayered communications architecture in mind (which currently exists only in theory, but is to be implemented in the near future). In order to implement the protocol within the currently existing software in the test vehicles, no fundamental changes in the protocol were necessary. However, certain abilities of the multilayered architecture had to be added into the existing software. As this work is just entering the test stage, results are not available yet.

The control structure for automated vehicles in an Automated Highway System is based on the idea of multiple-surface sliding control. The "upper" surface determines a desired net torque while the "lower" surface determines the required throttle angle or brake pressure needed to achieve the desired torque. Chapter 4 presents an upper surface control law for performing longitudinal transition maneuvers. The maneuvers use desired

velocity trajectories which are based on maintaining safety and comfort throughout the maneuver. The control law chosen is a sliding controller due to the non-linearities in the dynamics and the uncertainties in the parameters. The controller was implemented into experimental vehicles and tested at highway speeds. Control laws for join maneuvers were successfully implemented. Quantitative results have been presented.

Keywords: IVHS, AVCS, CICC, Longitudinal Control, Transition Maneuver, platoon

Executive Summary

The research presented in this report represent two different methods of vehicle control on an automated highway system (AHS). Chapter 2 covers the development of the Cooperative Intelligent Cruise Control (CICC). CICC is designed so that it is capable of operating under a "mixed" traffic flow, where some vehicles are equipped with CICC and others are manually operated. It implements automatic throttle and brake control along with a simple vehicle to roadside communication. CICC acts somewhat like a traditional cruise control with the added feature of collision avoidance, and it requires the driver to control the lateral motion of the vehicle. The roadside infrastructure provides the vehicle with information (such as maximum velocity) which can be controlled by the roadside to optimize traffic flow. The control system would accept a desired velocity input from the driver, and range and range-rate inputs from on-board sensors in order to achieve velocity tracking and collision avoidance.

The control system under CICC is designed using three control modules and one switching module. The cruise control module tries to follow a desired velocity trajectory based on input from the driver. The maximum velocity suppression module attempts to follow a desired velocity trajectory based on a maximum velocity set by the roadside. The distancing control module attempts to maintain an intervehicular spacing so as to avoid collision with the vehicle in front. The switching module selects one of the outputs of the control modules and applies it to the vehicle. Of the three control modules, the effectiveness of the distancing control module in particular was verified through simulation. These simulations utilized a seven degree-of-freedom nonlinear vehicle model, and included scenarios of vehicle following, "catching up", and of a vehicle "cutting in" in front of the cruise controlled vehicle. Comparing it to nominal headway controllers, CICC was found to provide both better ride quality, and improved collision avoidance both nominally, and in the presence of sensor noise. Although acceleration of the preceding vehicle is not obtainable as a direct measurement, acceleration estimation (AE) is shown to improve collision avoidance using CICC. In spite of its promising performance characteristics, it is still unclear how this method can improve the capacity of highways, and further research is needed in this area.

The second methodology considers operations involving platoons of vehicles. **A** platoon is a group of closely spaced vehicles under some sort of automatic control, and can exchange information through a wireless intervehicle communication system. Basic longitudinal platoon maneuvers consist of the platoon join and split maneuvers. Chapter **3** addresses the need to reconfigure the communication system during one of these maneuvers, and chapter 4 addresses the control algorithms required to physically carry out the maneuvers.

The communications system within a platoon can be thought of as a local area network (LAN), with each vehicle occupying an address in this network. During a platoon maneuver, the addresses in the LAN need to be reconfigured to reflect the changes in the platoon. Assuming that the communications channel between vehicles is not perfect and transmissions can be lost, any reconfiguration protocol must verify that all messages have been received before changing the addresses in the LAN. The consequence of failing to do so is that vehicles can become "lost" and be unable to communicate with any vehicle, either in its "old" platoon or the "new" one(s). Since the stability of the spacing control algorithm relies on the information transmitted through the communication system, this loss of communications is unacceptable from a control standpoint. Even assuming that the LAN reconfiguration proceeds smoothly, any reconfiguration of a wireless channel has the possibility of disrupting communications for a short time simply because radios need a finite time to switch between channels. In order to minimize the effect of this disruption on the ability of the control algorithm to maintain spacing, it is desirable to minimize the duration of this channel disruption. A protocol was developed for the platoon split maneuver, using a series of handshaking messages and timers to ensure that all vehicles have the necessary information to successfully reconfigure the LAN once the maneuver is complete. A protocol for the join maneuver is still under development, since this maneuver presents special problems in that "first contact" between previously independent platoons. Current radio hardware limits actual testing to two vehicles, since the radios currently in use have only one channel.

To execute the longitudinal transition maneuvers involved in these platoon maneuvers, a vehicle must generate a desired trajectory, and then have a control algorithm which can successfully follow the desired trajectory. In a split maneuver, the objective is to move two closely spaced vehicles apart. For a join maneuver, the objective is to move two distant vehicle together. The join maneuver in particular presents an increased danger of collision since it involves moving vehicles towards each other. The desired velocity trajectories that a vehicle would follow in one of these maneuvers were designed such that if a collision were to occur for whatever reason, the relative velocity at impact would be limited to some v_{safe}. It was found that trajectories designed using only this condition may require more time to complete than was desired, so a modified velocity trajectory was designed using multiple stages that would optimize both safety and time. With the desired trajectory established, a sliding mode controller was designed to follow this desired trajectory. The full maneuvers required the use of two control algorithms. The "transition" control law tracked the desired velocity profile for that particular maneuver. When it was determined that the transition was complete (i.e. the vehicles were far enough apart, or close enough together, depending on which maneuver was being executed), control was handed off to a follower control law, which maintained the desired spacing between

the two vehicles. This system was field tested using two Fort Lincoln Towncars equipped with throttle and brake actuators, radar, and wheel speed sensors. The results showed a comfortable ride quality, and acceptable tracking of the velocity profiles during the execution of the maneuvers.

CONTENTS

List of Figures

Chapter 1 Introduction

There are two methods to meet the increasing demand for the transportation on highway :

(1) constructing new highways and expanding existing lanes.

(2) to increase the capacity of the most used highways , to decrease traffic congestion and improve safety and air quality.

Because of the extremely cost and some tight restriction such as limited space and stringent environmental stands of the first method, the second one by using highly developed mechanical and electrical technologies to reach the goal becomes more attractive. An automated highway system called Intelligent Vehicle Highway System (IVHS) is now being developed under the direction of the Federal Highway Administration on this point of view. The main idea is the traffic flow rate is expected to be raised by means of closer packing of vehicles on highways while the safety and comfortbility being improved. The California Partner for Advanced Transit and Highway Systems (PATH) has been developed since 1986 to improve the efficiency of highways. It focuses on system management issues, inter-vehicle communications , vehicle control , and actuator and sensor development for IVHS applications. The studies on vehicle control are called AVCS (Advanced Vehicle Control System), and PATH has been working on platooning, which consists of automated throttle and brake control(longitudinal), steering control (lateral), and inter-vehicular communications. One platoon consists of as many as fifteen or twenty vehicles and the inter-vehicular distance is very small. Under this system, the relative velocity or the impact of a rear end collision in a platoon is small enough to be absorbed by bumpers, and the inter-platoon distance is sufficiently large so as to avoid entire platoons colliding with each other. In AVCS, it has been shown that platooning can achieve a greater capacity on highways but it needs substantial support from infrastructures to make its automatic controls possible, such as

those about tight vehicle following, steering, merge, and split [1] Such integrated infrastructure support as that PATH requires does not seem to be available soon while the demands for improving the efficiency of highways have been urgent issues under recent congested and stressful highway environments.

An approach to AVCS in [2] called "Cooperative Intelligent Cruise Control System" (CICC System) has been proposed. It includes an automatic throttle and brake control, i.e. longitudinal control, and simple infrastructure-vehicle communication. CICC is supposed to be used in a mixed flow where both automated vehicles and manually operated vehicles exist on highways at the same time. Infrastructures give certain kinds of information to each CICC vehicle to control traffic flow. CICC is designed so that it works as a conventional cruise control system when there no vehicles ahead or only some vehicles in the distance. It also works as a distancing-control system when vehicle ahead come into a certain range. Morever, CICC can achieve good riding comfort even if there exist vehicles
that suddenly cut in front, while it can effectively avoid rear end collisions with stopping vehicles and those that brake suddenly.

The spacing control approach requires information from other vehicles to ensure non-propagation of errors down a platoon of vehicles. The analysis of the effect of an imperfect communications systems on the performance of the control law has been done. [3]

This final report is for MOU#99 Phase III of a three-year project . Based on the past year's research work, in Chapter 2 a CICC will be designed so that it satisfies the system requirements. The system includes several sub-modules such as cruise control, maximum velocity suppression, and distancing control. The process by which each control module is designed is also described. The simulation results using a non-linear vehicle model that has seven degrees of freedom will also be show. These simulations emphasize the capacity of CICC to avoid collisions while achieving good riding comfort.

Longitudinal transition maneuvers consist of a "merge" maneuver and a "split" maneuver. The splitting and merging of platoon(s) requires a reconfiguration of the communication network within the platoon(s). The reconfiguration of a local area network will result in a temporary disruption in communications due to the rearranging of vehicle addresses. The platoon should remain stable through this transitory period where no communication is present. This "downtime" should be as short as possible in order to allow the controller to maintain performance and spacing requirements within the platoon. In Chapter 3, a protocol for a platoon split maneuver has been developed and is being readied for testing.

When a vehicle wishes to perform longitudinal transition maneuvers it must generate a desired velocity trajectory that will allow it to successfully perform the maneuver and then have a control algorithm that ensures the vehicle follows the desired trajectory. In Chapter 4, a closed loop trajectory design is presented for both the join and split maneuver. **A** sliding control method was used to force the vehicle to follow the desired trajectory within an acceptable boundary layer even when the errors between the model parameters and the actual parameters were at a maximum. Once the control structure was developed, it was tested and verified using the Vehicle Dynamics Lab vehicle simulation *long_sim.c* Experiments were also performed to verify the trajectory designs and control laws. Quantitative results will be presented in this report.

Chapter 2
CICC System Design and Simulation

2.1 Introduction

The third chapter in [3]describes how CICC should be organized and what kinds of information is necessary to make CICC possible through some analytical works. As a result of these analyses, it was shown that CICC should use headway control for vehicle-following. As for infrastructure-vehicle communication, CICC will be given the information of a desired headway time, maximum velocity, and road-tire friction by infrastructures through wide-range communication. CICC should also contain a module which estimates the acceleration of a preceding vehicle, and the estimated acceleration will be used to improve the capacity of avoiding collisions. This chapter will show the detailed processes of designing CICC and the simulation results using a non-linear vehicle model.

This chapter is organized as follows. In Section 2.2, a CICC will be designed so that it satisfies the system requirements. The system includes several sub-modules such as cruise control, maximum velocity suppression, and distancing control. The process by which each control module is designed is also described. Section 2.3 will show the simulation results using a non-linear vehicle model that has seven degrees of freedom. These simulations emphasize the capacity of CICC to avoid collisions while achieving good riding comfort. Section 2.4 will be a concluding section and summarize the features of CICC system.

2.2 System Design of CICC

A CICC system contains several sub-systems, such as cruise control and distancing control, each of which will also be described. While each sub-system is designed to maintain the system stability, CICC achieves good riding comfort as well as sufficient capacity of avoiding collisions.

One of the inputs to CICC is inter-vehicular distance. Although the technology for this kind of sensors have not been fully established yet, it is assumed that such sensors for inter-vehicular distance can measure distances with a certain resolution and are not equipped with devices such as a scanning system to detect wide, horizontal areas. (Thus, the sensors measure distances in a fixed direction only.)

The output of CICC is supposed to be acceleration, and when it is installed in a real vehicle, the acceleration command should be translated to certain actuator commands such as throttle angle and brake torque. The process by which desired acceleration is translated to real actuator commands will be described in Section 2.3.

2.2.1 System Description

CICC is designed to include automatic throttle and brake (longitudinal) control as well as infrastructure-vehicle communication. Human drivers are supposed to control the steering. The information from infrastructures is desired headway time, vehicle's maximum velocity, and road-tire friction. CICC does not support inter-vehicular communication because the latter does not significantly improve performance when the percentage of vehicles under automated control is less than *50 %* [2,3].

CICC also works as a cruise control or a collision avoidance system based on information such as inter-vehicular distance, relative velocity, and so on. To provide good riding comfort for human drivers, CICC is designed to minimize the jerk not only in maneuvers under a specific mode but also during transitions to other modes, while protecting against collisions.

CICC consists of three control modules and one switching module presented in Fig. 2.2.1. The three control modules are cruise control, maximum-velocity suppression, and distancing control. In the switching module, CICC sends a control command to the throttle and brake controller based on the commands it receives from control modules. The function of each module is briefly described below.

a. Cruise Control Module

The cruise control module keeps a vehicle's velocity desired speed. The inputs to this module are the cruising velocity from drivers and vehicle's current velocity.

b. Maximum-velocity Suppression Module

The maximum-velocity suppression module keeps a vehicle's velocity smaller than the maximum specified by infrastructures. The inputs to this module are maximum velocity and vehicle's current velocity.

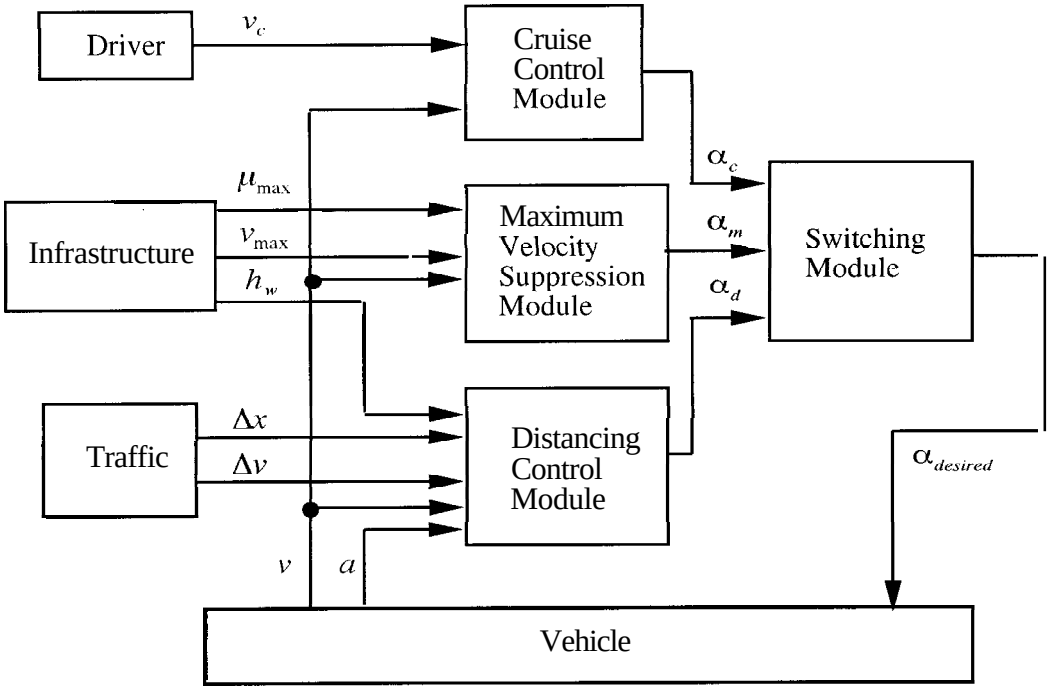

Fig. 2.2.1: System Diagram of CICC

c. Distancing-control Module

The distancing-control module keeps desired inter-vehicular distance (headway time) and avoids rear-end collisions. The inputs are desired headway time from infrastructures, and current inter-vehicular distance, relative velocity, current vehicle velocity, and vehicle acceleration.

d. Switching Module

The switching module sends commands to the throttle and brake controller based on commands it receives from each control module. The switching module also should be designed so as to keep the system stable.

2.2.2 Design of Cruise Control Module

Human drivers determine a desired velocity, and from the moment when a desired velocity, v_c, is given, the system defines the following velocity trajectory.

$$v_{desired}(t) = v(0) + (v_c - v(0))\left\{\frac{t}{T} - \frac{1}{2\pi}\sin\left(\frac{2\pi}{T}t\right)\right\} \qquad 0 \le t \le T \tag{2.2.1}$$

where $v(0)$ shows the vehicle's velocity at the moment when the cruise control begins, and T represents the settling time for smooth transition. T will be defined so that the maximum acceleration and jerk along the velocity trajectory are within the acceptable limit values. The maximum acceleration and jerk obtained from the velocity trajectory are expressed as follows:

$$a_{max} = \frac{2}{T}(v_c - v(0))$$

$$j_{max} = \frac{2\pi}{T^2}(v_c - v(0)) \tag{2.2.2}$$

Based on the sliding surface defined as

$$S = v_{desired}(t) - v \tag{2.2.3}$$

the desired acceleration is defined as

$$\alpha_c = (v_c - v(0))\left\{\frac{1}{T} + \frac{\lambda_c}{T}t - \frac{1}{T}\cos\left(\frac{2\pi}{T}t\right) - \frac{\lambda_c}{2\pi}\sin\left(\frac{2\pi}{T}t\right)\right\} + \lambda_c(v(0) - v) \tag{2.2.4}$$

where λ_c is the gain in sliding surface.

2.2.3 Design of Maximum-velocity Suppression Module

The maximum-velocity suppression module takes a step similar to that of cruise control module. Based on a given maximum velocity, v_{max}, a desired velocity trajectory is obtained as follows:

$$v_{desired}(t) = v(0) + (v_{max} - v(0))\left\{\frac{t}{T} - \frac{1}{2\pi}\sin\left(\frac{2\pi}{T}t\right)\right\} \qquad 0 \le t \le T \tag{2.2.5}$$

Thus, from the sliding mode control theory, a desired acceleration is defined as

$$\alpha_m = (v_{max} - v(0))\left\{\frac{1}{T} + \frac{\lambda_m}{T}t - \frac{1}{T}\cos\left(\frac{2\pi}{T}t\right) - \frac{\lambda_m}{2\pi}\sin\left(\frac{2\pi}{T}t\right)\right\} + \lambda_m(v(0) - v) \tag{2.2.6}$$

where λ_m is the gain in sliding surface. The maximum acceleration and jerk are calculated as

$$a_{max} = \frac{2}{T}(v_{max} - v(0))$$

$$j_{max} = \frac{2\pi}{T^2}(v_{max} - v(0)) \tag{2.2.7}$$

2.2.4 Design of Distancing Control Module

The block diagram of distancing control module is described in Fig. 2.2.2 This module consists of five sub-modules in order to realize good inter-vehicular distance tracking, collision avoidance, and riding comfort.

The nominal control module achieves good tracking, while the smoothing control module keeps good riding comfort for human drivers. The emergency control module is designed to avoid collisions when a vehicle is about to collide with other vehicles. The degree of emergency is introduced to determine whether a vehicle is in a danger of collisions. Based on this, the fuzzy switching module will generate a desired acceleration by calculating a weighted mean of the desired acceleration of each control module. The acceleration estimation module is used to estimated the acceleration of a preceding vehicle, and the estimated acceleration will be fed to the fuzzy switching module to improve the capacity of avoiding collisions. The design process of each sub-module will be described.

2.2.4.1 Nominal Control

The sliding surface for headway control is

$$S = \Delta x - L_0 - h_w v \tag{2.2.8}$$

where Δx is the inter-vehicular distance. With $\dot{S} = -\lambda S$, the desired acceleration of nominal control is defined as

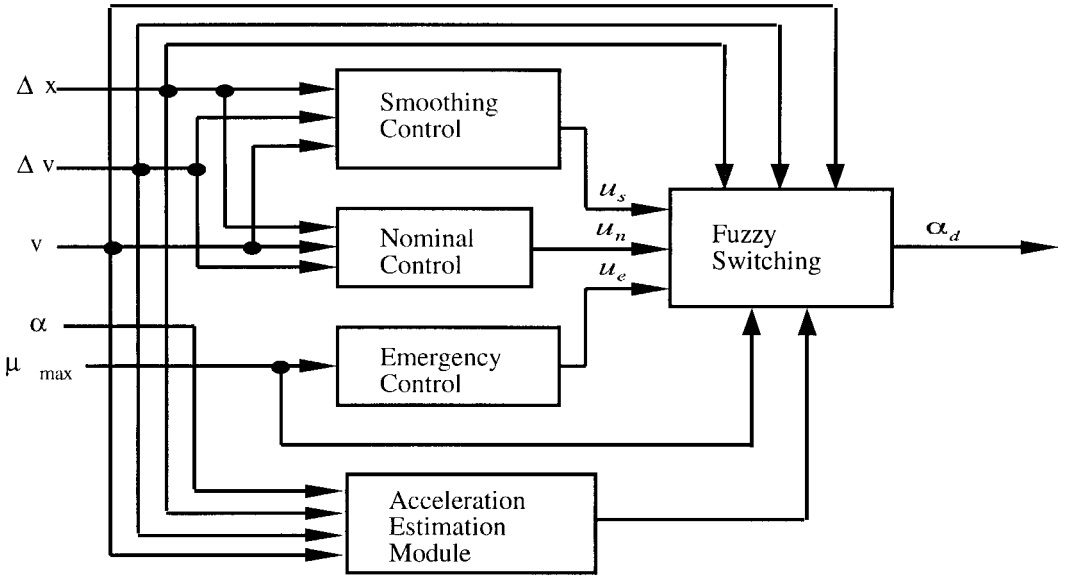

Fig. 2.2.2: Diagram of Distancing Control Module

$$u_n = \frac{1}{h_w}\left(\lambda\left(\Delta x - L_0\right) + \Delta v - \lambda h_w v\right) \tag{2.2.9}$$

where Δv is the relative velocity or time derivative of Δx.

2.2.4.2 Smoothing Control

Equation (2.2.9) guarantees that inter-vehicular distance converges uniformly to a desired headway distance, but due to some disturbances, such as sensor noise and the cut-in or cut-out of preceding vehicles, substantial jerk may exist and degrade riding comfort. To reduce this jerk, the smoothing controller introduces some low-pass filters and defines define a desired acceleration as

$$u_d = \frac{1}{h_w}\left(\lambda_1 x_{rf} + v_{rf} - \lambda_1 h_w v_f\right) \tag{2.2.10}$$

where

$$\begin{aligned} \dot{x}_{rf} + C_1 x_{rf} &= C_1(\Delta x - L_0) \\ \dot{v}_{rf} + C_2 v_{rf} &= C_2 \Delta v \\ \dot{v}_f + C_3 v_f &= C_3 v \end{aligned} \tag{2.2.11}$$

and where Δx and Δv are inter-vehicular distance and relative velocity, respectively. C_1, C_2, and C_3 indicate low-pass filter bandwidths which smooth desired acceleration or reduce jerk during maneuvering. This controller is stable if the low-pass filter bandwidth is chosen properly (In [2] Appendix **B** 1).

In case of $C_1 = C_2 = C_3 = C$, Eq. (2.2.10) represents an actuator with the first-order delay, whose time constant is *1/C*. As was shown in [2, 3], the first-order delay of an actuator should be small enough to satisfy string stability, whose condition is described as

$$C \geq \frac{2(1 + h_w \lambda_1)}{h_w} \tag{2.2.12}$$

To achieve good riding comfort, however, jerk should be kept small not only on one sliding surface but also at the moment when a transition is made to control mode, such as from cruise control to distancing control. In general, jerk can be expressed as

$$j = \frac{d(u_d - \alpha)}{dt} \approx \frac{u_d - \alpha_0}{\Delta t} \tag{2.2.13}$$

where Δt and α_0 are sampling time for control and desired vehicle acceleration at the last sampling, which is sent to a throttle and a brake controllers. Note that α_0 may be defined by control modules other than the smoothing one. To suppress a jerk value during mode transitions, define another sliding surface as

While Eq. (2.2.11) is useful in reducing the jerk that results from small disturbances such as sensor noise, sudden and large disturbances result from vehicle maneuvering, such as cut-in and cut-out. In these cases, riding comfort may be compromised because the low-pass filters can provide controllers with extremely large values. To maintain this comfort in cases of cut-in and cut-out, saturation nonlinearities or limiters should be added to low-pass filters for the sensors that detect inter-vehicular distance and relative velocity. (Limiters are illustrated in Fig. 2.2.3 [4,5].)To prevent filtered inter-vehicular distance from drifting off while a vehicle is catching up a preceding

one, the limiter is turned on only when an inter-vehicular distance is larger than the desired headway distance.

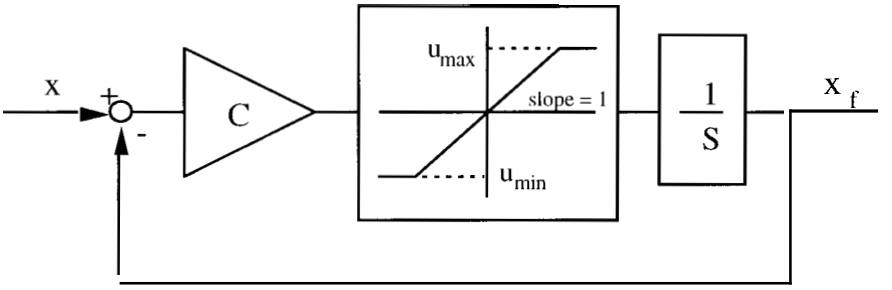

Fig. 2.2.3: Limiters for Low Pass Filters

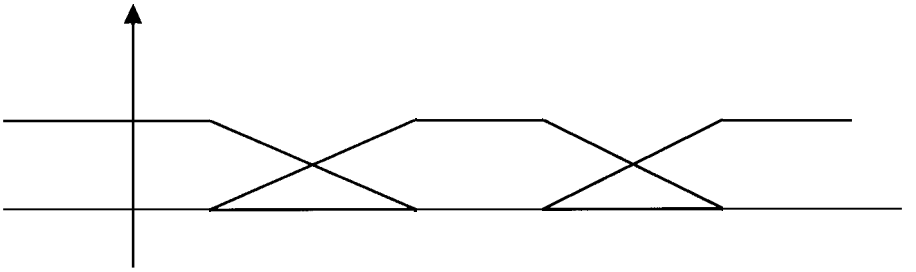

Fig. 2.2.5: Membership Functions for Fuzzy Switching

$$S_2 = u_d - \alpha \tag{2.2.14}$$

and $\dot{s}_2$ corresponds to jerk. Then let

$$S_2 = -\lambda_2 S_2 \tag{2.2.15}$$

Equation (2.2.15) implies that $\dot{S}_2$ is zero if S_2 is zero. By designing the control mode so that if will be switched to smoothing control from other modules when S_2 changes its positive sign to negative, the equation ensures that jerk will always be zero during mode transitions to the smoothing control. From Eqs. (2.2.14) and (2.2.15), "desired jerk" is defined by

$$\dot{\alpha}_{desired} = \dot{u}_d + \lambda_2 S_2 \tag{2.2.16}$$

Applying the zero-order hold assumption,

$$\dot{\alpha}_{desired} = \frac{u_s - \alpha_0}{\Delta t} \tag{2.2.17}$$

By letting $a = u_s$, desired acceleration of the smoothing controller, which satisfies Eq. (2.2.15), is defined as

$$\begin{aligned} u_s &= \frac{1}{1+\lambda_2 \Delta t}\left\{\alpha_0 + \Delta t\left(\dot{u}_d + \lambda_2 u_d\right)\right\} \\ &= \frac{1}{1+\lambda_2 \Delta t}\alpha_0 \\ &+ \frac{\lambda_1 \Delta t}{1+\lambda_2 \Delta t}\frac{1}{h_w}\left\{(\lambda_2 - C_1)x_{rf} + C_1(x_p - x)\right\} \\ &+ \frac{\Delta t}{1+\lambda_2 \Delta t}\frac{1}{h_w}\left\{(\lambda_2 - C_2)v_{rf} + C_2(v_p - v)\right\} \\ &- \frac{\lambda_1 \Delta t}{1+\lambda_2 \Delta t}\left\{(\lambda_2 - C_3)v_f + C_3 v\right\} \end{aligned} \tag{2.2.18}$$

The system under this desired acceleration is also stable (In [2] Appendix B2). As time approaches infinity, the relation between desired accelerations defined by Eq. (2.2.10) and those by Eq. (2.2.18) is expressed in the discrete-time domain as

$$(1 + \lambda_2 \Delta t - z^{-1})(u_{sk} - u_{dk}) = 0 \tag{2.2.19}$$

The desired acceleration in Eq. (2.2.18) converges to the acceleration in Eq. (2.2.10) at steady state.

2.2.4.3 Emergency Control

The emergency controller works to avoid collisions under emergency situations, such as during severe cut-in and sudden, hard braking of preceding vehicles. In these cases, this controller commands the maximum deceleration, which is the maximum friction ratio between tires and the ground. This information is supposed to be relayed by the infrastructure, the reason for this is that a vehicle needs information about the friction of

roads where vehicles will be decelerated. Thus, the desired acceleration of an emergency controller is simply defined as follows:

$$u_c = -\mu_{max}\, g \tag{2.2.20}$$

2.2.4.4 Fuzzy Switching

From the three desired acceleration commands described above, the fuzzy-switching module generates the desired acceleration, which will be fed into the throttle and brake controllers. The desired acceleration is defined according to the degree of emergency: if the vehicle is judged to be performing a normal maneuver, the switching module picks up the smoothing control; if the vehicle is about to collide, it picks up the emergency control.

Based on the R-Rdot analysis[6], the degree of emergency is determined by

1) For $\dot{R} < 0$,

$$a_{em} = \frac{-d_1 + \sqrt{d_1^2 + \dfrac{2\dot{R}^2}{\mu_{max}\, g} d_2}}{2 d_2} \mu_{max}\, g \tag{2.2.21}$$

where

$$d_1 = R - h_w v_p - L_0$$
$$d_2 = (h_w - h_0) v_p + L_0 \tag{2.2.22}$$

2) For $\dot{R} > 0$ *and* $R < h_w v + L_0$,

$$a_{em} = -\frac{R - h_w v - L_0}{(h_w - h_0) v_p + L_0} \mu_{max}\, g \tag{2.2.23}$$

3) For $\dot{R} > 0$ *and* $R \geq h_w v + L_0$,

$$a_{em} = 0 \tag{2.2.24}$$

where h_0 and v_p denote the minimum headway time, which corresponds to $a_{em} = \mu_{max} g$ at zero relative velocity and the velocity of a preceding vehicle. The degree of emergency has the dimension of acceleration, and Fig. 2.2.4 illustrates the degree of emergency on an R-Rdot diagram with $h_w = 0.7\,\text{sec}, h_0 = 0.1\,\text{sec}, v_p = 10\,\text{m/sec}$, and $L_0 = 1\,\text{m}$. In the figure, Line **A** represents conditions in which the acceleration command is zero according to **Eq.** (2.2.9). Similarly, Line B represents conditions in which the acceleration command is equal to the maximum deceleration. Line C corresponds to the steady state of headway control where the inter-vehicular distance is identical to the desired headway distance.

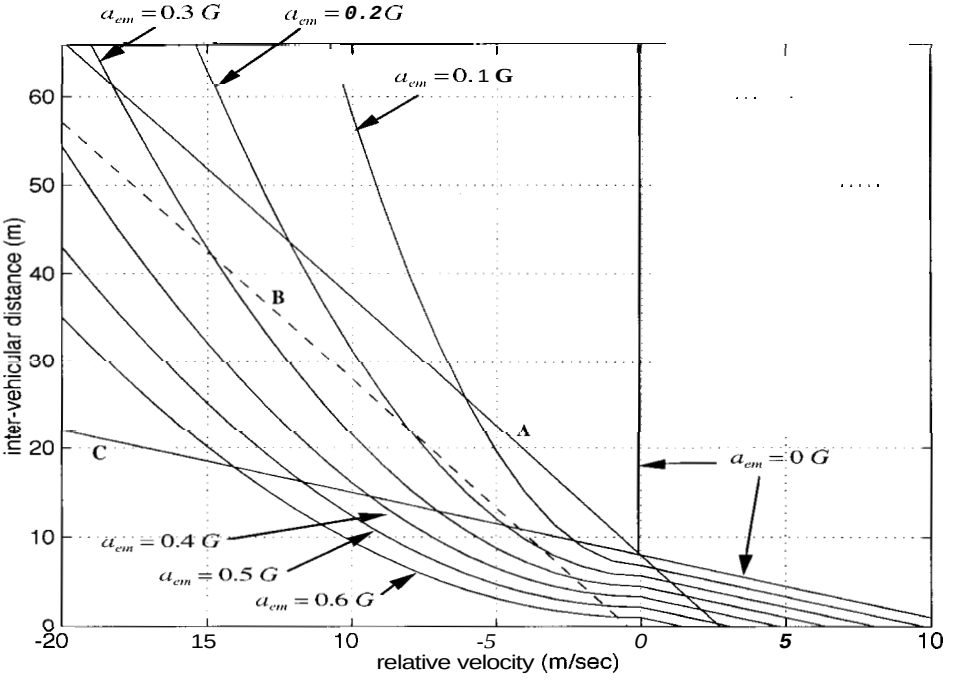

Fig. 2.2.4: Degree of Emergency

Based on the degree of emergency, the desired acceleration is derived from

$$\alpha_d = f_1 u_s + f_2 u_n + f_3 u_e \qquad (2.2.25)$$

where f_1, f_2, and f_3 are membership functions for fuzzy switching defined in Fig. 2.2.5. If the degree of emergency is smaller than a_1, the fuzzy-switching module will output smoothing-control acceleration. If the degree of emergency is between a_1 and a_2, the output will be an intermediate value between smoothing-control and nominal-control

accelerations. The system under the control input of Eq. (2.2.25) is stable (In [2] Appendix B*3)*.

With this fuzzy switching, the controller can achieve good riding comfort when vehicles are under usual vehicle-following. It also tracks the desired headway distance more precisely as the R-Rdot state is far from the desired steady state. It will avoid collisions when vehicles are about to do so with preceding ones in accordance with the R-Rdot diagram shown in Fig. 2.2.4.

2.2.4.5 Estimating Acceleration

As was demonstrated in [2,3], collision avoidance is dependent on the acceleration of preceding vehicles, and estimating their acceleration can improve the performance of distancing control. To do this, the acceleration-estimation module determines this acceleration in order to adjust the fuzzy switching. The adjustment will be made based on the following equation,

$$a'_{em} = a_{em} - \hat{\alpha}_p \tag{2.2.26}$$

where a'_{em} and $\hat{\alpha}_p$ are a modified degree of emergency and the estimated acceleration of a preceding vehicles, respectively. The fuzzy-switching module is supposed to use the modified degree of emergency instead of the nominal one. Then, Eq. (2.2.26) indicates that if a preceding vehicle is accelerating, the fuzzy-switching module promotes greater riding comfort, and that if a preceding vehicle is decelerating, it will promote more precise tracking.

The fastest and easiest way to calculate the acceleration of a preceding vehicle is to differentiate its velocity. This method, however, is not adequate for real implementations, because preceding vehicle's velocity can't be measured directly. Because this vehicle velocity has to be calculated from the summation of the following vehicle's velocity and its relative velocity, noise and delay must exist. Moreover, since the cut-in and cut-out of preceding vehicles results in discontinuity of information about the preceding vehicle, the differentiation does not work well under normal operation.

Then, another approach will be chosen here using detection filter. The general concept and the design procedure of detection filter are introduced in[7,8]. The detection filter is a kind of observer, which is specially designed to generate residuals due to errors of input. The residuals are zero when no error inputs exist, and each error induces a unique direction in measurement residual. For the acceleration-estimation module, the

detection filter is used for determining the acceleration by dealing with it as an unknown error.

The dynamics of CICC system can be described as

$$\dot{X} = \begin{vmatrix} 0 & 1 & -1 \\ 0 & 0 & 0 \\ 0 & 0 & 0 \end{vmatrix} X + \begin{vmatrix} 0 & 0 \\ 1 & 0 \\ 0 & 1 \end{vmatrix} \begin{bmatrix} \alpha_p \\ \alpha \end{bmatrix} \equiv A\,X + B\,u$$

$$y = \begin{vmatrix} 1 & 0 & 0 \\ 0 & 1 & -1 \\ 0 & 0 & 1 \end{vmatrix} X \equiv C\,X \tag{2.2.27}$$

where $X = [x_p - x, v_p, v]^T$, α_p is the preceding vehicle's acceleration, and α is the vehicle's acceleration. Thus, this is a two-input and three-output system. Since the current acceleration of vehicles is known to the CICC controller, the acceleration of preceding vehicles can be dealt with as system errors or faults. Note that there are five possible sources of errors: the preceding vehicle's actuator, the following vehcle's actuator, the inter-vehicular distance sensor, the relative velocity sensor, and the velocity sensor of vehicles. By following the process of detection-filter design (In [2] Appendix C1), the dynamics of errors or the residuals of the system due to error inputs can be expressed as

$$\dot{\tilde{X}} = (A - D_F\,C)\,\tilde{X} + [-B \vdots D_F]\,n_e$$

$$\mathrm{E} = C\,\tilde{X} + [0 \vdots I]\,n_e \tag{2.2.28}$$

where n_e, D_F, and I are the error-input vector, the gains of observer (or detection filter), and the identity matrix, respectively. The error-input vector is defined as

$$n_e = [\mu_1, \mu_2, \mu_3, \mu_4, \mu_5]^T \tag{2.2.29}$$

where entries correspond to a preceding vehicle's actuator error, a following vehicle's actuator error, an inter-vehicular distance sensor error, a relative-velocity sensor error, and a vehicle-velocity sensor error, respectively. Figure 2.2.6 presents observed error responses due to step inputs of each error. Figure 2.2.6 (a) displays step responses for a preceding vehicle's actuator error, and Fig. 2.2.6 (b) shows step responses for a following vehicle's actuator error, and so on. The gains of detection filter for Figs. 2.2.6 are defined as $\lambda_0 = \lambda_1 = \lambda_2 = 6.28\ \mathrm{rad/sec}$ in [2] Appendix C1. Since observer gains are chosen so

that the output due to each error input appears in a distinct direction on each observed error, each error input will result in different patterns of observed errors.

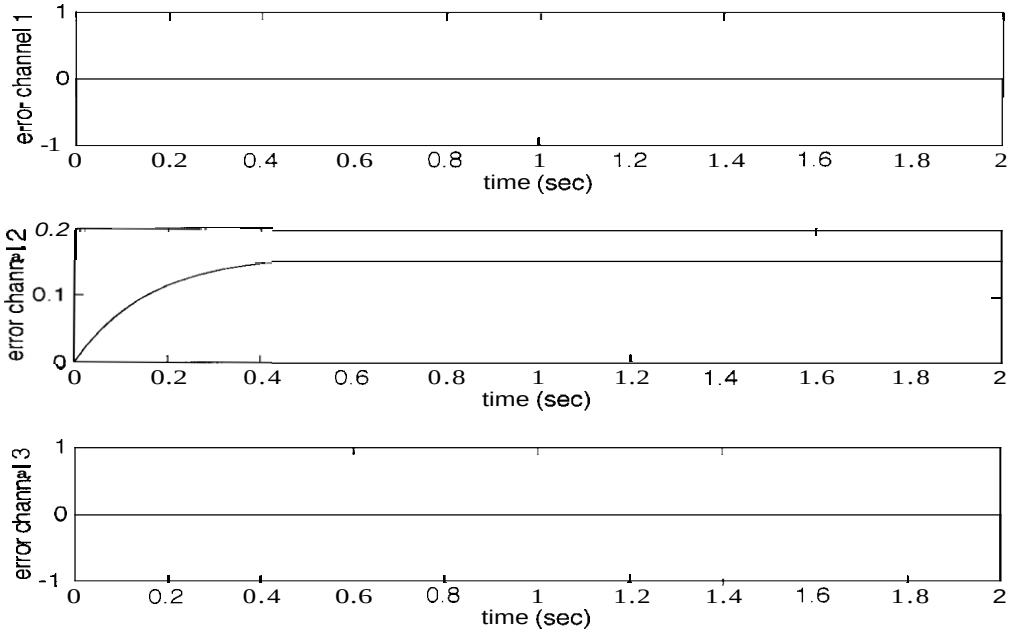

Fig. 2.2.6 (a): Detection Filter Errors due to Preceding Vehicle's Actuator Error

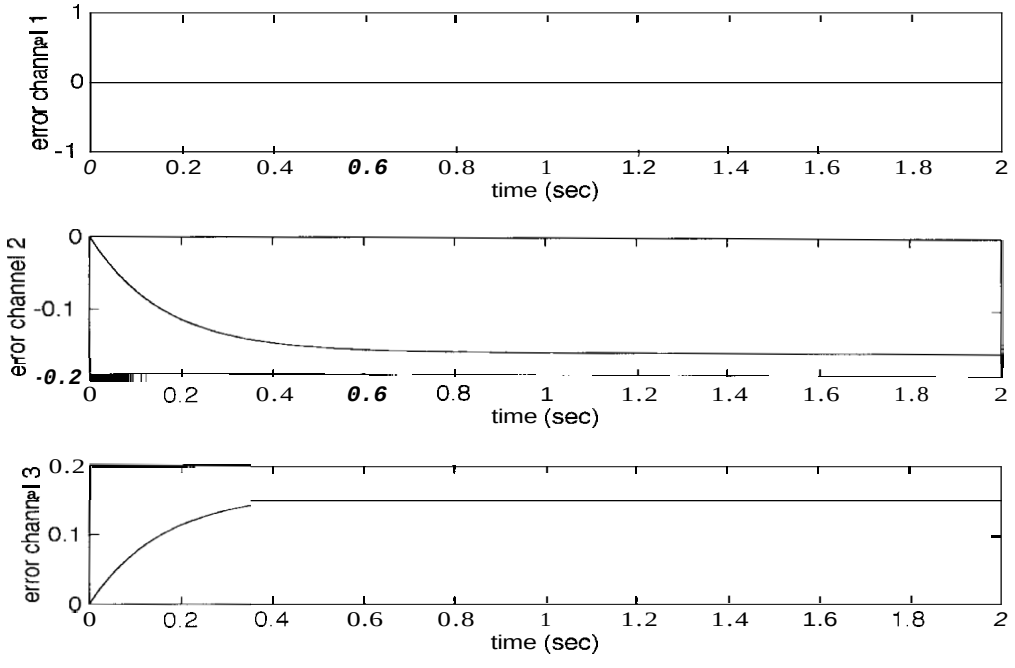

Fig. 2.2.6 (b): Detection Filter Errors due to Following Vehicle's Actuator Error

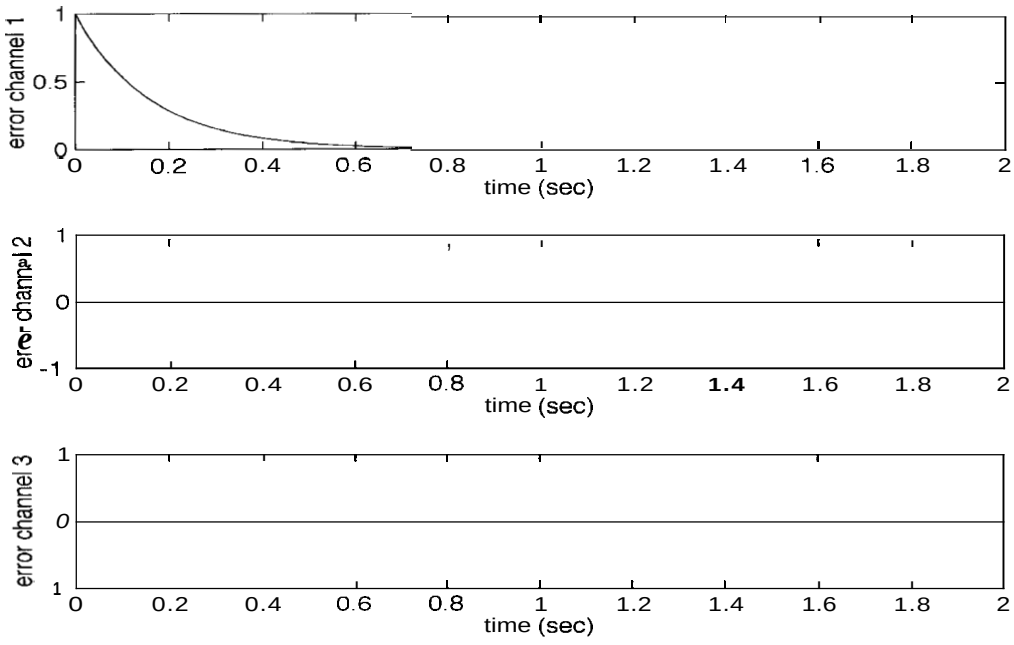

Fig. 2.2.6 (c): Detection Filter Errors due to Error of Distance Sensor

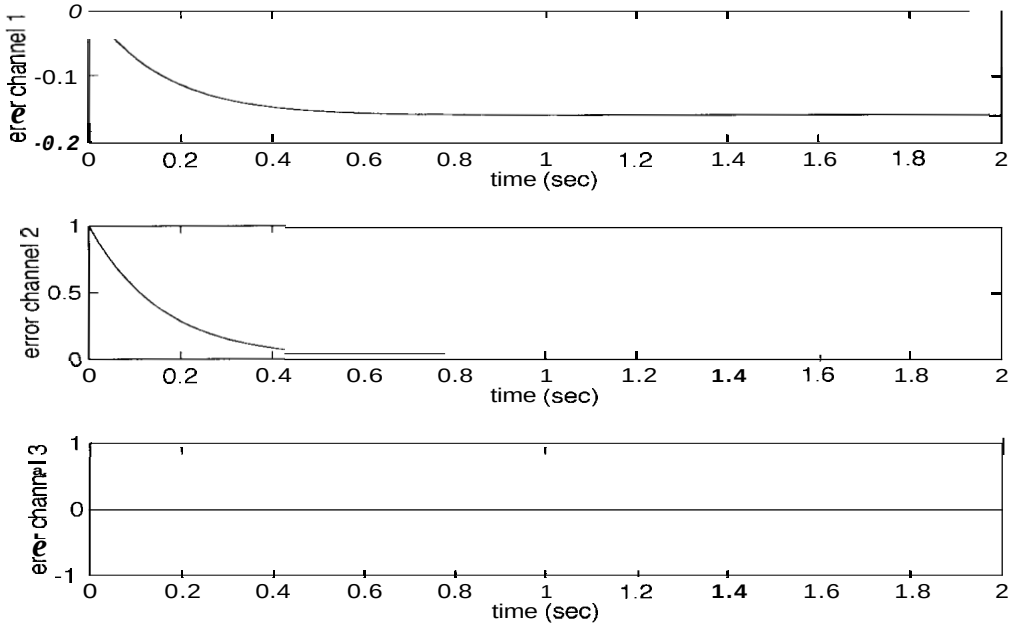

Fig. 2.2.6 (d): Detection Filter Errors due to Error of Relative Velocity Sensor

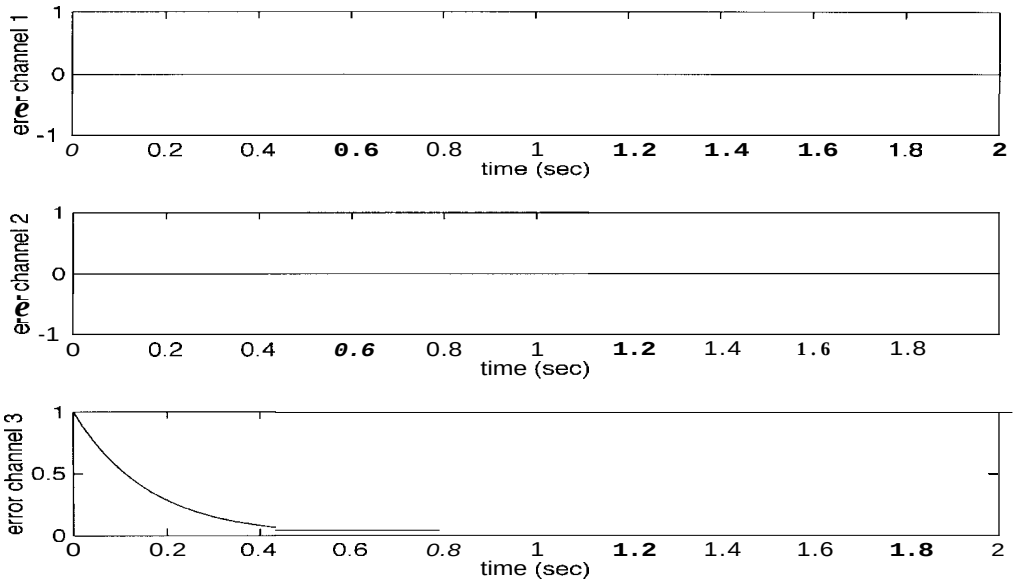

Fig. 2.2.6 (e): Detection Filter Errors due to Error of Vehicle Velocity Sensor

The effects of preceding-vehicle acceleration appear only in the second error channel at steady states. Since the effects of vehicle actuator errors also exist in the second channel at steady state, preceding vehicle acceleration can be estimated as

$$\begin{aligned}\alpha_{est} &\equiv p(\varepsilon_2 + \varepsilon_3) \\ &= \frac{p}{s+p}\mu_1 + \frac{ps}{s+p}(\mu_4 + \mu_5)\end{aligned} \tag{2.2.30}$$

where p is a gain defined as $\lambda_0 = \lambda_1 = h$, $= p$, and ε, and ε, indicate the second and the third error channels, respectively. Equation (2.2.30) shows that the estimated acceleration includes information about relative-velocity sensor errors and vehicle-velocity sensor errors in high-frequency domains. Since the errors of a vehicle's velocity sensor may be small or can be modeled as Gaussian distributed noise, simple low-path filters can suppress their influences on the estimation of acceleration. However, because the errors of a relative-velocity sensor can be huge, especially in cases of cut-in and cut-out, Eq. (2.2.30) can't be directly used for estimation of acceleration. Since a preceding vehicle is replaced by another one suddenly in these cases, the relative velocity abruptly jumps to a certain value, and an extraordinarily large spike should appear in the estimated acceleration defined in Eq. (2.2.30). However, since the change of relative velocity can be modeled as

a step input in cases of cut-in, the duration time of spikes can be predicted by the cut-off frequency, p. If cut-in and cut-out are detected, the influences of sudden changes in relative velocity can be avoided by turning off the acceleration estimation mechanism during a fixed period of time. Since the effects of cut-in and cut-out are mainly observed in the first and second error channels, these channels will be utilized as cut-in detectors. The process of designing a cut-in detector is described in [2] Appendix C2.

2.2.5 Switching Module

The switching module selects one of the outputs of the three modules, cruise control , maximum velocity suppression , and distancing control. Each module is defined based on a residual that represents margins of safety for each control objective. For example, if velocity is larger than the desired cruise velocity, Eq. (2.2.3) takes a negative value, which can be interpreted as a dangerous state; if the velocity is too large in comparison with the inter-vehicular distance, Eq. (2.2.8) becomes negative, which is also a dangerous situation from the viewpoint of collision-avoidance.

In CICC control, a switching module will utilize the "choose-minimum" logic among three outputs, which can be simply written as

$$\alpha_{\text{desired}} = \min\left(\alpha_c, \alpha_m, \alpha_d\right) \tag{2.2.31}$$

where $a,$, $a„$ and α_d are the outputs of cruise control, maximum velocity suppression, and distancing modules, respectively. Eq. (2.2.31) guarantees that the desired acceleration is always smaller than or equal to the output of each module. Since a smaller desired acceleration will result in a smaller velocity and a smaller required inter-vehicular distance, this logic works to prevent all of the residuals from becoming negative, or to keep them within the safe region.

The system under the desired acceleration defined by this switching module is also stable since it picks up one of the outputs of the three stable modules.

2.3 Performance of CICC

In this Section, the performances of a CICC will be evaluated through simulations with a non-linear vehicle model. The vehicle model used in this section is the same as that presented in[9], which has been used for the simulations in the PATH project. This vehicle model contains several non-linearities to emulate real vehicle responses while eliminating excessive complexity. **A** simplified vehicle model to implement CICC will also be presented. When implementing a CICC, the robustness of CICC will be evaluated because there must exist some modeling errors.

The simulations consist of various scenarios on highways, such as catching-up and cutting-in, and, depending on these situations, the performance of a CICC will be compared with nominal headway control and with other CICC's, whose specific functions are turned off.

2.3.1 Vehicle Model for Simulation

To conduct simulations of intelligent cruise control systems, the dynamics of engine, vehicle velocity, and brake torque should be considered. In modeling these dynamics, to avoid needless complexity, models are developed based on several assumptions. For engine dynamics, it is assumed that the ideal gas law holds in the intake manifold, and the temperature of the intake manifold is constant. As for vehicle velocity dynamics, the drive axle is assumed to be sufficiently rigid, while brake dynamics are modeled as a first order delay system.

2.3.1.1 State Variables

The vehicle model consists of seven degrees of freedom as follows:

- m_a mass of air in intake manifold expressed in kg
- w_e engine speed in rad/sec
- v car velocity in m/sec
- x car position in m
- w_w wheel speed in rad/sec
- T_{br} brake torque in Nm
- α_T throttle angle in degree

2.3.1.2 State Equations

The dynamics of the intake manifold are given by

$$\dot{m}_a = \dot{m}_{a\_in} - \dot{m}_{a\_out} \tag{2.3.1}$$

$$P_m V = m_a \bar{R} T_m \tag{2.3.2}$$

where $\dot{m}_{a-in}$ *and* $\dot{m}_{a\_out}$ are the mass flow rates through the throttle valve, and into the cylinders, respectively. P_m, V, and T_m are the intake manifold pressure, volume, and temperature. $\bar{R}$ is the gas constant. The relation between $\dot{m}_{a\_in}$ and P_m is

$$\dot{m}_{ai} = MAX \cdot TC(\alpha_T) \cdot PRI\left(\frac{P_m}{P_a}\right) \tag{2.3.3}$$

where MAX is a constant that depends on the size of the throttle body. $TC(\alpha_T)$ is the throttle characteristic that is the projected area of air flow as a function of the throttle angle α_T. PRI is the pressure influence function, and P_a is the atmospheric pressure. $\dot{m}_{a\_out}$ is defined by

$$\dot{m}_{a\_out} = \bar{\dot{m}}_{a\_out}(w_e, P_m) \tag{2.3.4}$$

where $\bar{\dot{m}}_{a\_out}$ is a table, look-up map for air flow rate which is unique to each engine. The engine rotational dynamics are

$$\dot{w}_e = \frac{T_{net} - T_{pump}}{J_e} \tag{2.3.5}$$

where T_{net}, T_{pump}, and J_e are net engine torque, torque-converter pump's torque, and the engine's inertia, respectively. T_{net} and T_{pump} are defined by

$$T_{net} = \bar{T}_{net}(w_e, P_m)$$

$$T_{pump} = \bar{T}_{pump}\left(\frac{w_w}{R^* w_e}\right) \tag{2.3.6}$$

where $\bar{T}_{net}$, $\bar{T}_{pump}$, and R^* are table, look-up maps for net torques of the engine and torque-converter pump, and the total gear ratio from engine to wheels, respectively. The delay time for the engine to generate torque is also taken into account. The wheel dynamics are

$$\dot{w}_w = \frac{T_T / R^* - T_{wl}}{J_W} \tag{2.3.7}$$

where T_T, T_{wl}, and J_w are torque-converter turbine's torque, resistance between wheels and the ground, and the inertia of wheels. T_T also is defined by

$$T_{pump} = \bar{T}_{turbine}\left(\frac{w_w}{R^* w_e}\right) \tag{2.3.8}$$

where $\bar{T}_{turbine}$ is the table, look-up map for torque-converter turbine's torque. The brake dynamics are described by

$$\dot{T}_{br} = \frac{T_{brc} - T_{br}}{\tau_b} \tag{2.3.9}$$

where T_{brc} and τ_b are the commanded brake torque and the time constant for the brake actuator. The dynamics for vehicle speed are given by

$$\dot{v} = \frac{F_{tr} - C_a v^2 - f_f}{M} \tag{2.3.10}$$

where T_{tr}, C_a, f_f, and M are traction force, drag coefficient, rolling resistance, and vehicle mass, respectively. F_{tr} is given by

$$F_{,,} = K_r \,.\mathrm{sat}\left(\frac{i}{i_{max}}\right) \tag{2.3.11}$$

where K_r i, and i_{max} are longitudinal tire stiffness, slip ratio between wheels and the ground, and the maximum slip ratio, respectively. In the simulation, a stepping motor will be used as the throttle-angle actuator, and its dynamics are given by

$$\dot{\alpha} = sat\left(\frac{\dot{\alpha}_c}{\dot{\alpha}_{max}}\right) \tag{2.3.12}$$

where $\dot{\alpha}_c$ and $\dot{\alpha}_{max}$ are the time derivative of the commanded throttle angle and the maximum actuator speed. In addition to all of these variables, it is assumed that the gear position of transmission is in third gear throughout the simulations.

The parameters used in simulations are as follows:

$$V = 4.470\ x\ 10^{-3}\ m^3,\ \boldsymbol{R} = 8.278\ x\ 10^{-3},\ T_m = 310.93\ K,$$
$$\boldsymbol{MAX} = 684.11\ kg/sec,\ P_a = 100.0\ \boldsymbol{k}\ Pa,\ J_e = 0.263\ kgm^2,$$
$$R^* = 0.3058,\ J_w = 2.565\ kg\,m^2,\ \tau_b = 0.1\ sec,$$
$$C_a = 0.534\ N\,sec^2/m^2,\ f_f = 167\ \boldsymbol{N},\ \boldsymbol{M} = 2148\ kg,$$
$$K_r = 81030.0\ N,\ \dot{\alpha}_{max} = 450.0\ deg/sec$$

2.3.2 Implementation of Controller

In this section, the process of implementing CICC on the non-linear model described above will be discussed. As a matter of fact, the desired acceleration generated by CICC should be translated into the real control commands such as throttle angle and brake torque. To do this, the non-linear model should be simplified based on some additional assumptions.

In implementing CICC, it is assumed that there are no modeling errors about the dynamics of engine torque, throttle-angle actuator, and brake torque. However, there can still exist some modeling errors about vehicle dynamics. Then, even after CICC is implemented successfully, it is necessary to consider the effects of modeling errors because they can degrade the stability of the system. As a result, it will be shown that the system will be still stable with the existence of certain modeling errors.

2.3.2.1 Simplified Vehicle Model for Controller

Since some information about a vehicle is not available for controllers, the vehicle model needs to be modified in order to comply with control laws. Therefore, the model is simplified base on the following assumptions:

1) The torque converter is locked.

2) There is no slip between wheels and the ground.

Since the vehicle's velocity is proportional to its engine speed, the differential equation of vehicle's velocity dynamics is expressed as

$$\dot{v} = R^* h \dot{w}_e = \frac{R^* h}{J_{eff}} \left[T_{net} - R^* T_{br} - R^* h f_f - C_a R^{*3} h^3 w_e^2 \right] \tag{2.3.13}$$

where T_{net}, h, and J_{eff} are net engine torque, effective tire radius, and total inertia of the vehicle, respectively. J_{eff} is defined by

$$J_{eff} = J_e + J_w R^{*2} + M(R^* h)^2 \tag{2.3.14}$$

where J, , J_w, and M are engine inertia, wheel inertia, and vehicle mass, respectively. Then, the desired net engine torque is chosen as

$$T_{net\_desired} = R^* h \dot{w}_e = \left[R^* T_{br} + R^* h f_f + C_a R^{*3} h^3 w_e^2 \right] + \frac{J_{eff}}{R^* h} \alpha_{desired} \tag{2.3.15}$$

where $\alpha_{desired}$ is the desired acceleration of vehicles. By substituting Eq. (2.3.15). for Eq. (2.3.13), vehicle acceleration is identical to the desired one. The desired pressure of the intake manifold can be found in a table, look-up map, that is,

$$P_{md} = \overline{P}_m \left(w_e, T_{net\_desired} \right) \tag{2.3.16}$$

where P_{md} and $\overline{P}_m(\ ,)$ denote the desired pressure of the intake manifold and the table, look-up map, respectively. From Eq. (2.3.2), the air mass in the intake manifold is defined by

$$m_{a\_desired} = \frac{P_{md} V}{\overline{R} T_m} \tag{2.3.17}$$

Based on a sliding surface as $S = m_{a\_desired} - m_a$, by applying $\dot{S} = -\lambda_t S$,

$$\alpha_{T\_command} = TC^{-1}\left[\frac{\dot{m}_{a\_out} + \dot{m}_a + \lambda_t\left(m_{a\_desired} - m_a\right)}{MAX\ PRI\left(P_m/P_a\right)}\right] \tag{2.3.18}$$

If commanded throttle angle is smaller than the minimum throttle angle α_{T_0}, braking should occur. In this case, from Eq. (2.3.13), the desired brake torque is defined as

$$T_{br\_desired} = \frac{J_{eff}}{R^{*2}h}\alpha_{desired} - \frac{1}{R^*}\left[T_{net} + R^* h f_f + C_a R^{*3} h^3 w_e^2\right] \tag{2.3.19}$$

Similarly, based on a sliding surface as $S = T_{br\_desired} - T_{br}$, by applying $\dot{S} = -\lambda_b S$,

$$T_{br\_command} = T_{br} + \tau_b\left(\dot{T}_{br\_desired} + \lambda_b\left(T_{br\_desired} - T_{br}\right)\right) \tag{2.3.20}$$

The commanded throttle angle and brake torque defined in Eqs. (2.3.18) and (2.3.20) yield

$$x = \alpha_{desired} \tag{2.3.21}$$

2.3.2.2 Robustness of Modeling Error

If there are no modeling errors, Eqs. (2.3.18) and (2.3.20) yield the desired acceleration; however, the effects of modeling errors in the system should be confirmed during implementation. For example, in Eq. (2.3.15), rolling resistance, vehicle inertia, and drag coefficient are not always constant, and it is difficult to know the precise values in real situations. Thus, the robustness of the system due to changes in parameters should be considered.

Assume that there are some modeling errors in these three parameters,

$$f_{f\_real} = f_f + \Delta f_f$$

$$J_{eff\_real} = J_{eff} + \Delta J_{eff}$$

$$C_{a\_real} = C_a + \Delta C_a \tag{2.3.22}$$

where the subscript, *real* denotes the real values, and Δ represents modeling errors. By substituting Eq. (2.3.22) for Eq. (2.3.15), the real acceleration that the controller can achieve is expressed as

$$\alpha_{real} = \frac{J_{eff}}{J_{eff\_real}} \alpha_{desired} - \frac{R^{*2} h^2}{J_{eff\_real}} \Delta C_a v^2 - \frac{R^{*2} h^2}{J_{eff\_real}} \Delta f_f \tag{2.3.23}$$

In Eq. (2.3.23), the third term does not affect the system's stability, although it does yields an offset of the outputs. However, the first and second terms may undermine the system's stability since the first term changes the A matrix, and the second term is a nonlinear residual.

With real acceleration defined in Eq. (2.3.23), the linearized system with smoothing control can be expressed in a form similar to that in [2] Appendix C1 as

$$\dot{X} = \begin{bmatrix} -C & 0 & 0 & -C & 0 \\ 0 & -C & 0 & 0 & -C \\ 0 & 0 & -C & 0 & C \\ 0 & 0 & 0 & 0 & 1 \\ \frac{\lambda_1}{r h_w} & \frac{1}{r h_w} & -\frac{\lambda_1}{r} & 0 & 0 \end{bmatrix} X + \begin{bmatrix} 0 \\ 0 \\ 0 \\ 0 \\ k \Delta C_a v^2 \end{bmatrix} \equiv A X + f(X) \tag{2.3.24}$$

where $r = \frac{J_{eff\ real}}{J_{eff}}$ and $k = \frac{R^{*2} h^2}{Jeff\_real}$. The terms for external inputs and the modeling error of rolling resistance are deleted in Eq. (2.3.24) because they do not affect the system's stability. The system in Eq. (2.3.24) can be shown to be absolutely stable with a finite domain (in [2] Appendix D).

2.3.3 String Stability of the CICC System

The string stability of the CICC system should be maintained although the non-linear model contains some possible sources of string instability such as engine delay, throttle and brake-response delays, sensor delays, and wheel dynamics. Moreover, CICC includes low-pass filters for smoothing control, which can cause string instability. Then, first of all, it is necessary to check whether the CICC system maintains its string stability or not through a vehicle-following simulation.

In the simulation, a lead car travels with a velocity trajectory as shown in Fig. 2.3.1, and thirty vehicles will follow it with zero initial spacing error and zero initial relative velocity. The magnitudes of acceleration and deceleration of the lead car during changes in velocity are 1 m/sec^2. The desired headway time is 0.7 seconds, and the distance offset is 1 meter. As for controls, the sampling time is 0.02 seconds, the control gains are $\lambda = \lambda_1 = 0.45$ and $\lambda_2 = 1.0$, and the low-path filter bandwidth for smoothing is 1 Hz. By taking sensor delays in consideration, it is assumed that CICC defines the desired acceleration based on the sensor outputs at the previous sampling-time.

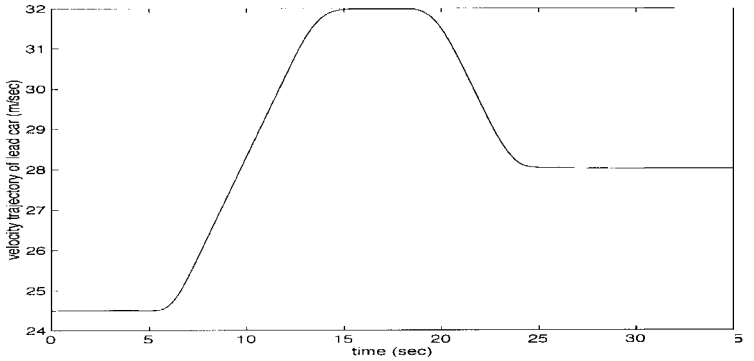

Fig.2.3.1: Velocity Trajectory of Lead Car

Figure 2.3.2 shows velocity trajectories, spacing errors, and throttle angles of the first, fifth, tenth, fifteenth, twentieth, and thirtieth following vehicles. As each vehcle's index increases, its trajectory becomes more dull, and the maximum spacing error also decreases. As for throttle-angle responses, their maximum increases with the first several vehicles, but they decrease if the vehicle index is larger than about ten. Thus, it can be concluded that CICC satisfies string stability.

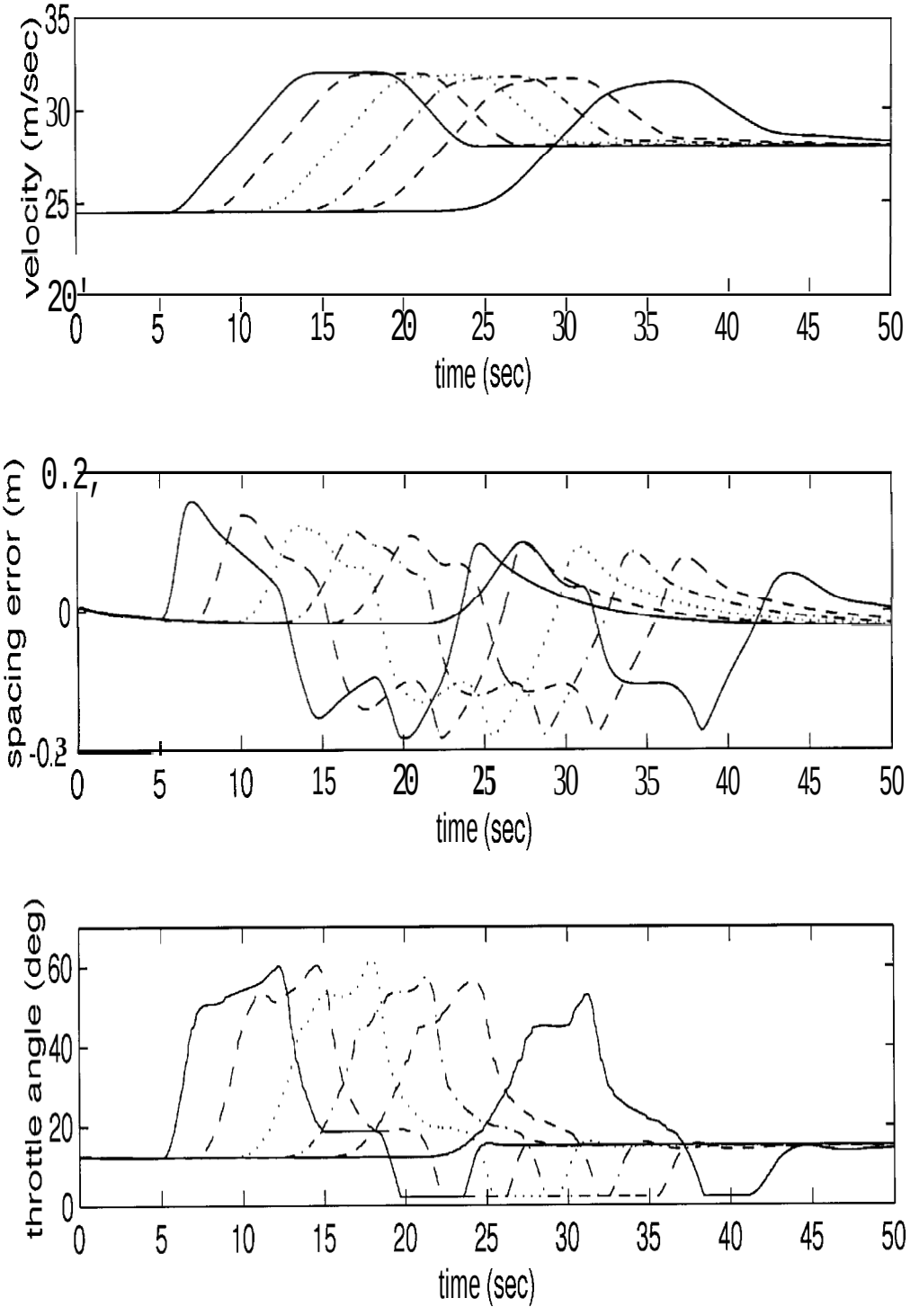

Fig. 2.3.2: String Stability of CICC in Non-linear Simulation

2.3.4 Effects of Smoothing Control on Sensor Noise

Noise on sensor outputs yields discontinuous controller outputs, which is especially damaging to the riding comfort of human drivers. In order to see the effects noise have on riding comfort, a simulation will be done with two distancing controllers: nominal and CICC.

Since noise comes from many sources, such as electric circuits and the dynamics of sensors, it is popular to model noise on sensor outputs as Gaussian distributed random variables. In real implementations, it is also known that the noise on inter-vehicular distance and relative velocity does not follow the Gaussian distribution, but for convenience sake, noise is supposed to be modeled as zero-mean Gaussian distributions in the following simulation.

The velocity trajectory of a lead car and other initial conditions are the same as those in the previous simulation, and the number of following vehicles is one. The standard deviation of sensor noise for simulation is 0.1 meters for an inter-vehicular distance sensor, 0.05 m/sec for a relative velocity sensor, and 0.05 m/sec for a velocity sensor.

The responses of a following vehicle with a nominal controller are illustrated in Fig. 2.3.3 (a), and those of a vehicle with a CICC are shown in Fig. 2.3.3 (b). These velocities look similar, but since the jerk becomes significantly smaller with a CICC, it certainly improves riding comfort.

Control inputs also show similar results; fluctuations in throttle angle are much smaller with CICC, and brake torque shows very smooth responses. **As** for nominal controller, many "spikes" exist in the brake torque responses. This is because nominal controller often brakes to compensate for the large noise of sensors. These spikes should be avoided because they result in "chattering" from a brake actuator.

Figure 3.4 shows the spacing errors of both controllers. Although riding comfort has been improved with CICC, spacing errors do not increase much. Moreover, in the case of a nominal controller, there exists an offset in spacing-error response, which results from spikes on the brake torque.

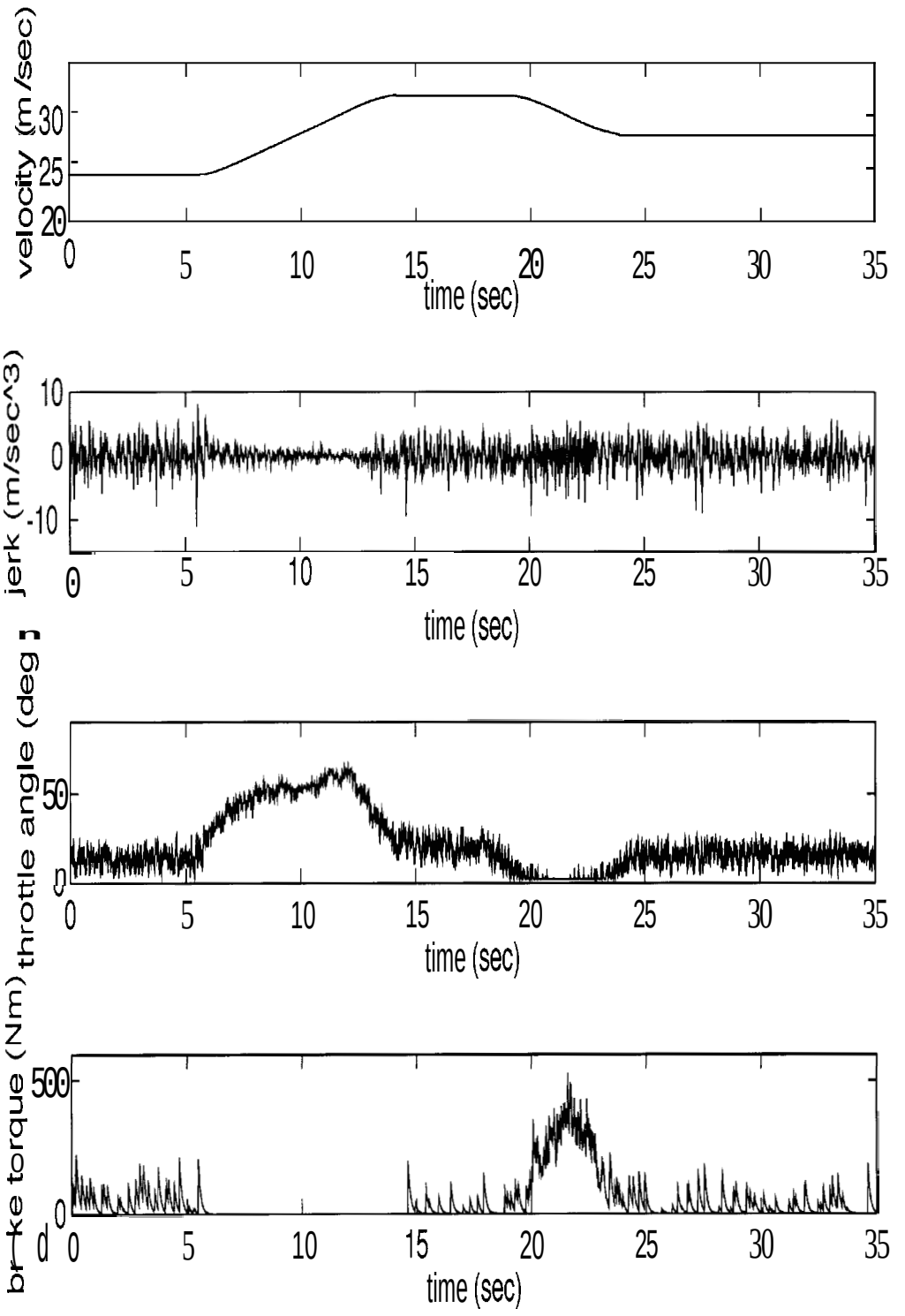

Fig. 2.3.3 (a): Transient Responses with Nominal Controller

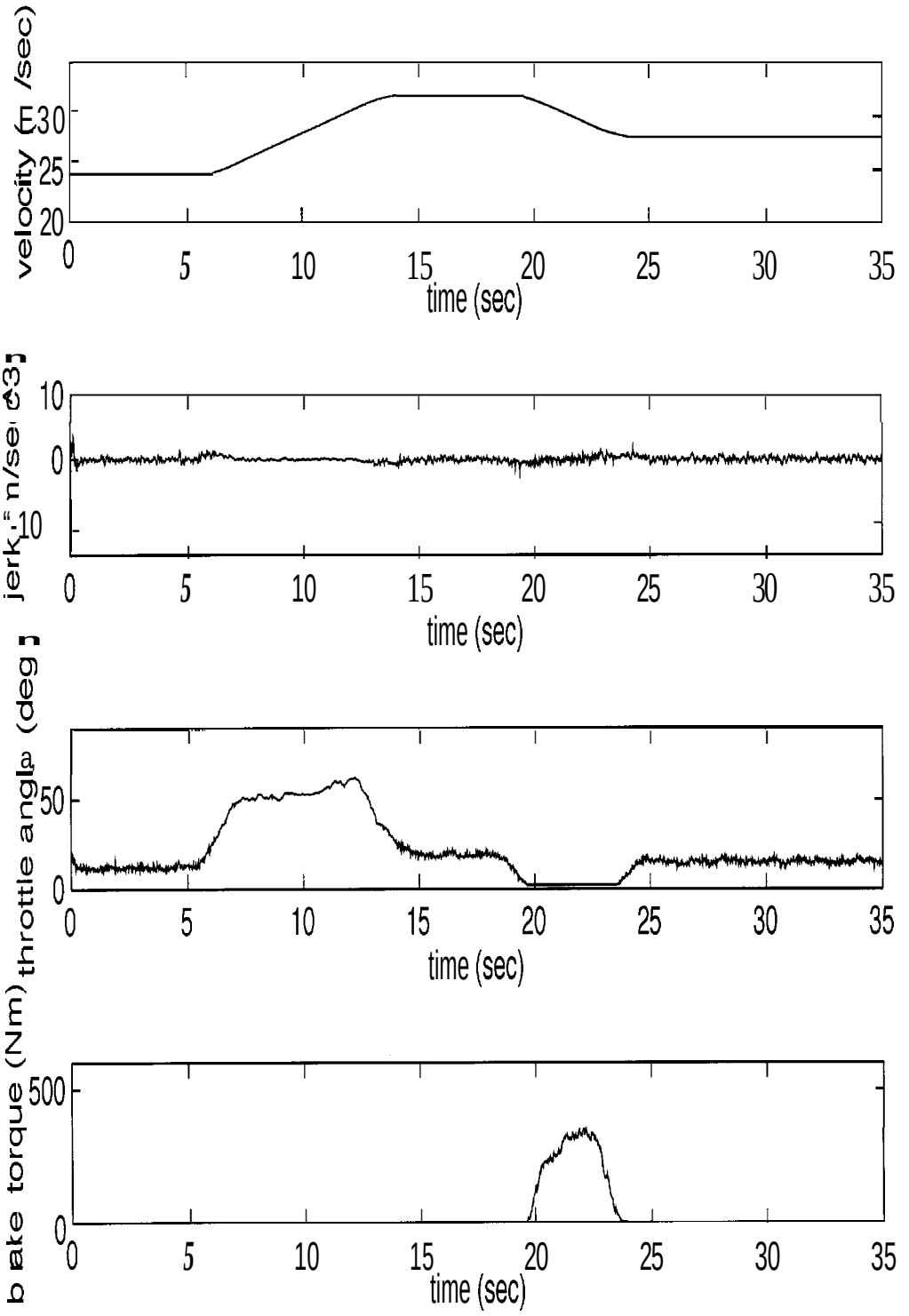

Fig. 2.3.3 (b): Transient Responses with CICC

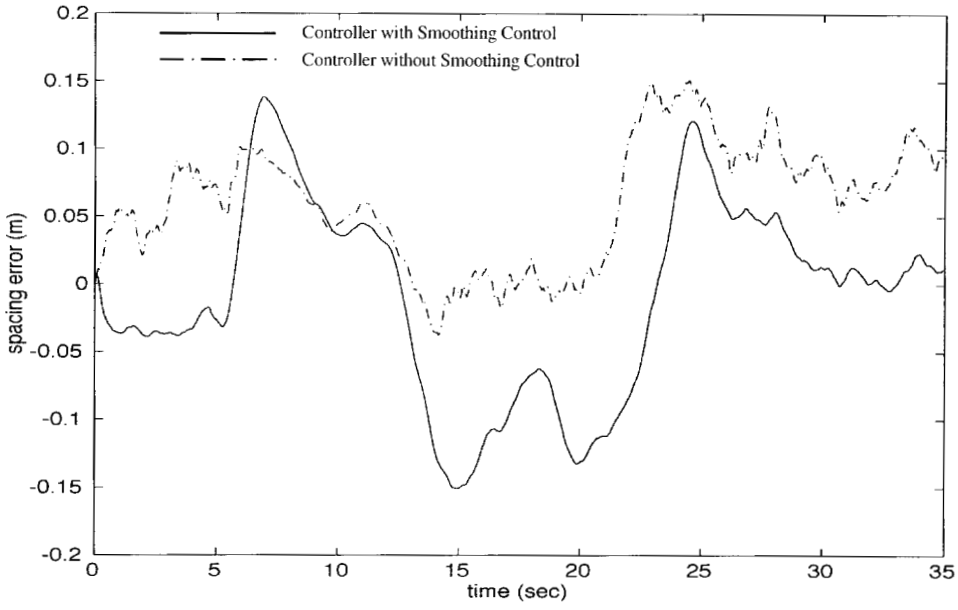

Fig. 2.3.4 : Spacing Errors

2.3.5 Effects of Smoothing on Mode Switching

Since CICC systems automatically change one control mode from one to another, maneuvering during these transitions must be smooth for human drivers. **A** mode transition occurs, for example, when two vehicles are far away initially, and a following vehicle is faster than a preceding one. To see the differences in jerk responses, a catch-up case is simulated for nominal controller and CICC.

The velocity of a preceding vehicle is supposed to be constant, 10 $dsec$, throughout the simulation. The initial velocity of a following vehicle is 20 $dsec$ and the initial inter-vehicular distance is 70 m; the desired headway time is 0.7 seconds and the control gains, λ_1 and λ_2, are both 0.45. Since the desired headway distance is 15 meters initially, a following vehicle is under cruise control at first. Then, when it approaches a preceding vehicle, the control mode will change to distancing control at certain positions. The simulation results are presented in Fig. 2.3.5: Fig. 2.3.5 (a) shows the results of a nominal control, and Fig. 2.3.5 (b) describes those of a CICC. Each set of results consists of an R-Rdot diagram, acceleration, and jerk.

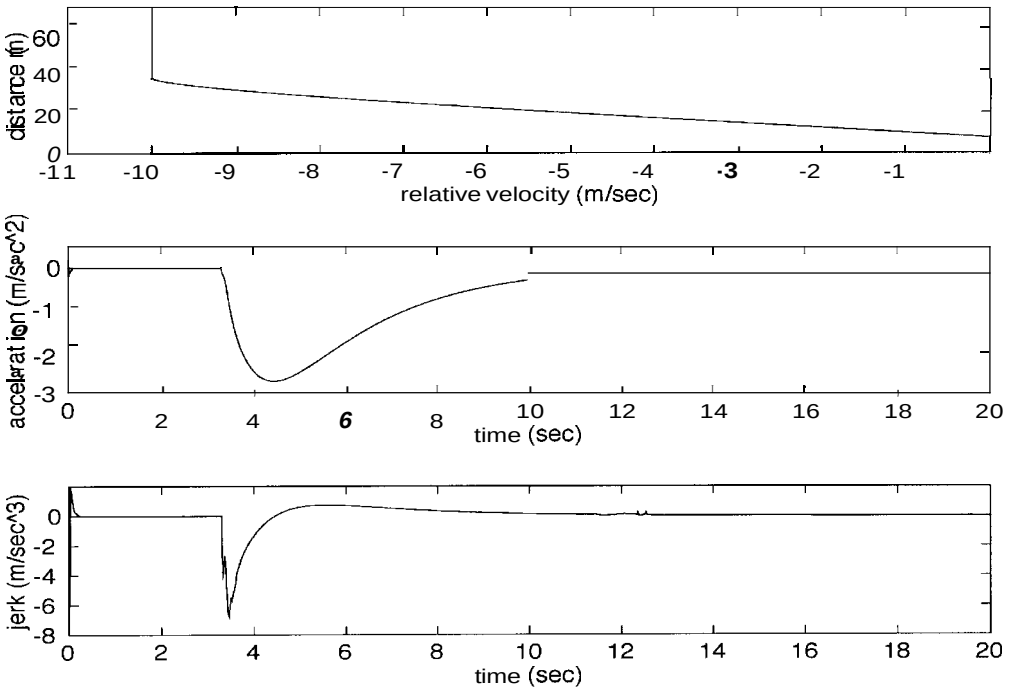

Fig. 2.3.5 (a) : Catching-up Case with Nominal Controller

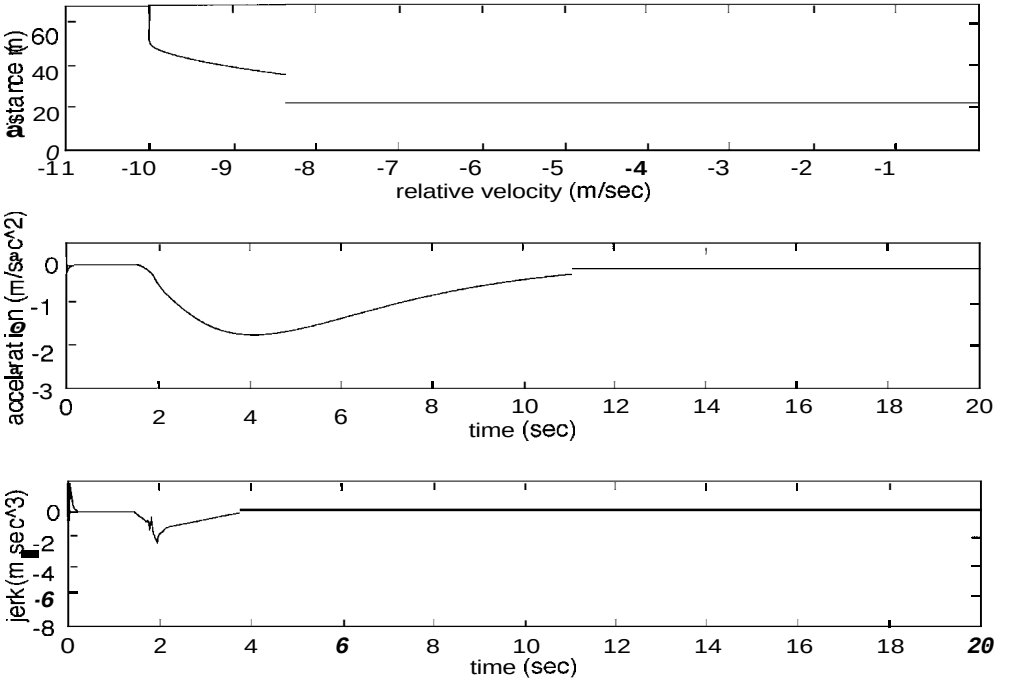

Fig. 2.3.5 (b) : Catching-up Case with CICC

From R-Rdot diagrams, it is observed that both controllers converge to the steady state without overshoot and that CICC begins to decelerate at a position further than the nominal controller. With CICC, the braking timing is also about two seconds earlier than nominal control, as shown in the figures on brake torque. Since braking begins earlier, the maximum deceleration and jerk of a CICC are smaller than those of a nominal controller. The maximum deceleration and jerk of a nominal control are 2.7 m/sec^2 and -6.8 m/sec^3, while those of a CICC are 1.7 m/sec^2 and -2.1 m/sec^3. Thus, CICC improves riding comfort for human drivers.

From R-Rdot diagrams, it is observed that both controllers converge to the steady state without overshoot and that CICC begins to decelerate at a position further than the nominal controller. With CICC, the braking timing is also about two seconds earlier than nominal control, as shown in the figures on brake torque. Since braking begins earlier, the maximum deceleration and jerk of a CICC are smaller than those of a nominal controller. The maximum deceleration and jerk of a nominal control are 2.7 m/sec^2 and -6.8 m/sec^3, while those of a CICC are 1.7 m/sec^2 and -2.1 m/sec^3. Thus, CICC improves riding comfort for human drivers.

2.3.6 Effects of Fuzzy Switching

One of the most common disturbances on highways is cut-in and cut-out. Since inter-vehicular distances and relative velocities change suddenly in these cases, acceleration will also change abruptly.

In cases of cut-in, both good riding comfort for human drivers and collision avoidance with preceding vehicles should be achieved by controllers. If a cut-in is mild, the controller should keep good riding comfort, and if a cut-in is steep, it should avoid collisions. To satisfy both requirements, fuzzy switching described in Section 2 is used in the following simulations.

A preceding vehicle is traveling at 30 $dsec$, and a following one traits behind it with 0.7-seconds of headway time and 1 meter of offset. The resulting headway distance is 22 meters. Another vehicle cuts in front of the following one with the same velocity at distances, 17, 12, 7, and 2 meters ahead it. Thus, the transient responses are modeled as unit-input responses of inter-vehicular distance. For a nominal controller, the control gain will be 0.45, and for CICC, $\lambda_1 = 0.45$ and $\lambda_2 = 1.0$. As for the limiters of inter-vehicular distance and relative velocity, $u_{max} = -u_{min} = 5$ is used for inter-vehicular distance and $u_{max} = -u_{min} = 3$ is used for relative velocity. The parameters for membership functions

of fuzzy-switchmg are $a_1 = 3, a_2 = 4.5, a_3 = 5$, and $a_4 = 5.5$. In the simulations, when another vehicle cuts in at a distance of x meters ahead a vehicle, "cut-in distance" is called as x meters.

Figure *2.3.6* (a) shows the results of nominal controller, and Fig. *2.3.6* (b) presents those of a CICC. Each set of figures consists of acceleration, an R-Rdot diagram, and spacing error during maneuvering.

The responses during the simulation indicate that when the cut-in distance is large, a CICC maintains good riding comfort. For example, with a 17-meter cut-in distance, the maximum acceleration of a CICC is smaller than that of a nominal controller, and the difference in riding comfort with a small cut-in distance is more significant in jerk responses, as shown in Fig. *2.3.6* (c). Since the nominal controller generates desired acceleration commands based on the current, inter-vehicular distance and relative velocity, the peak value of jerk is significantly larger, especially at the moment of cut-in. In contrast, the jerk of a CICC is quite smooth, and its peak value is about one-fifth of that of a nominal controller. As the cut-in distance decreases, the responses of a CICC become similar to those of a nominal controller. For example, with a cut-in distance of *2* meters, the transient responses of both controller are identical, except in the regions near to the steady state as shown in R-Rdot diagrams.

Thus, fuzzy switching achieves good riding comfort in cases of mild cut-in and collision avoidance in cases of hard cut-in. However, a trade-off exists. As seen in spacing errors, CICC takes more time to converge to the desired inter-vehicular distance than does a nominal controller. For reference, Fig. 2.3.7 shows the degree of emergency of CICC during maneuvering. Each line corresponds to a cut-in distance of 17, 12, 7, and *2* meters. As time approaches infinity, since all the trajectories come under the smoothing control according to the fuzzy switching rule, each response takes more time to reach the steady state.

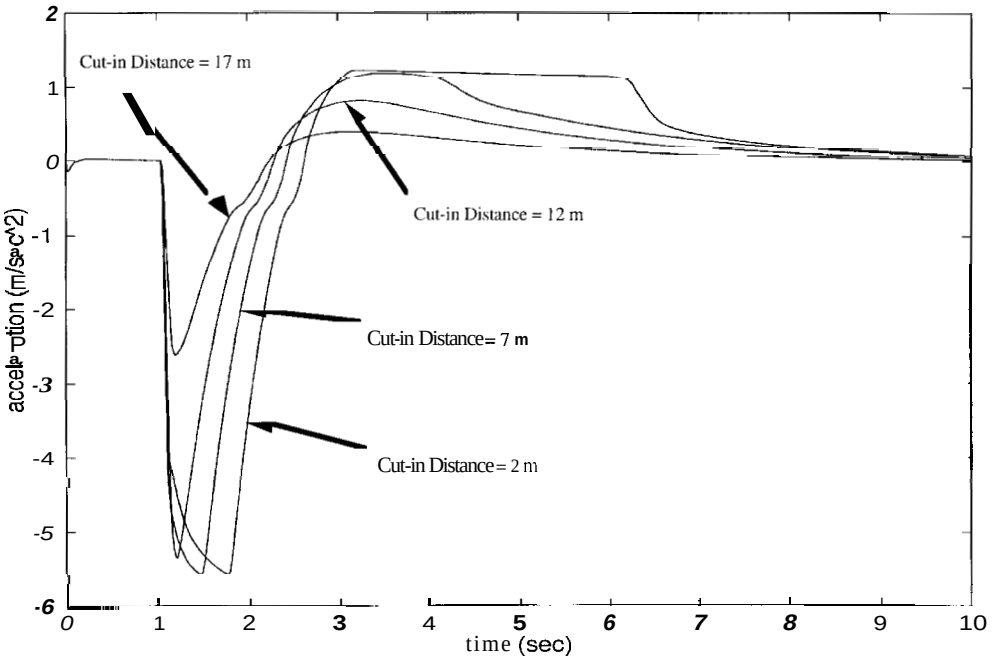

Fig. 2.3.6 (a): Cut-in Vehicle Response with Nominal Controller

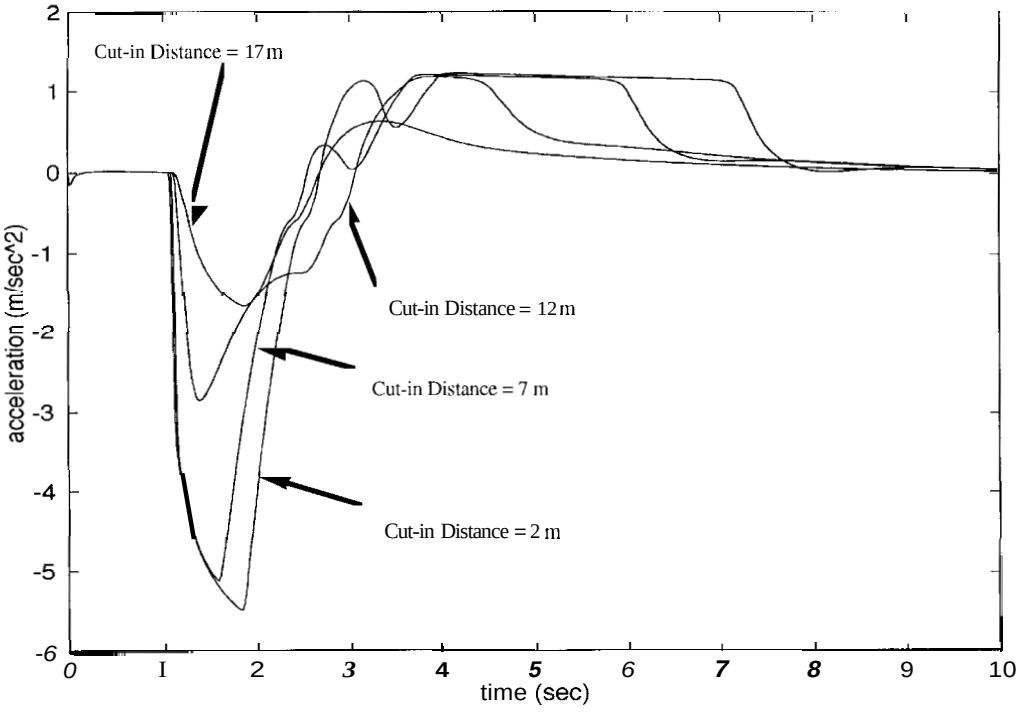

Fig. 2.3.6 (b): Cut-in Vehicle Response with CICC

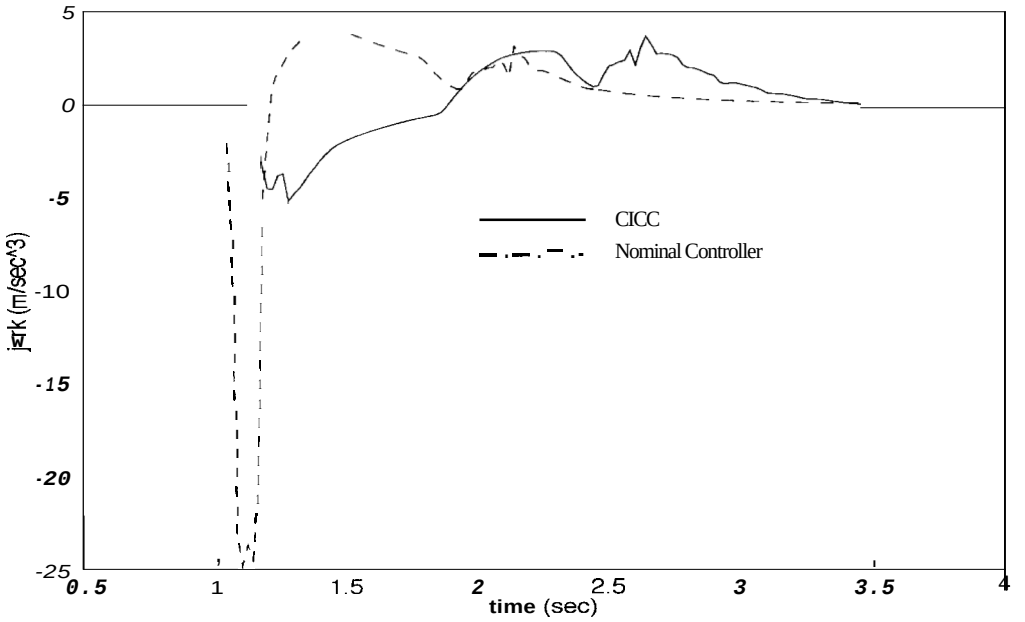

Fig. 2.3.6 (c): Jerk in the Case of a Five-meter Cut-in Distance

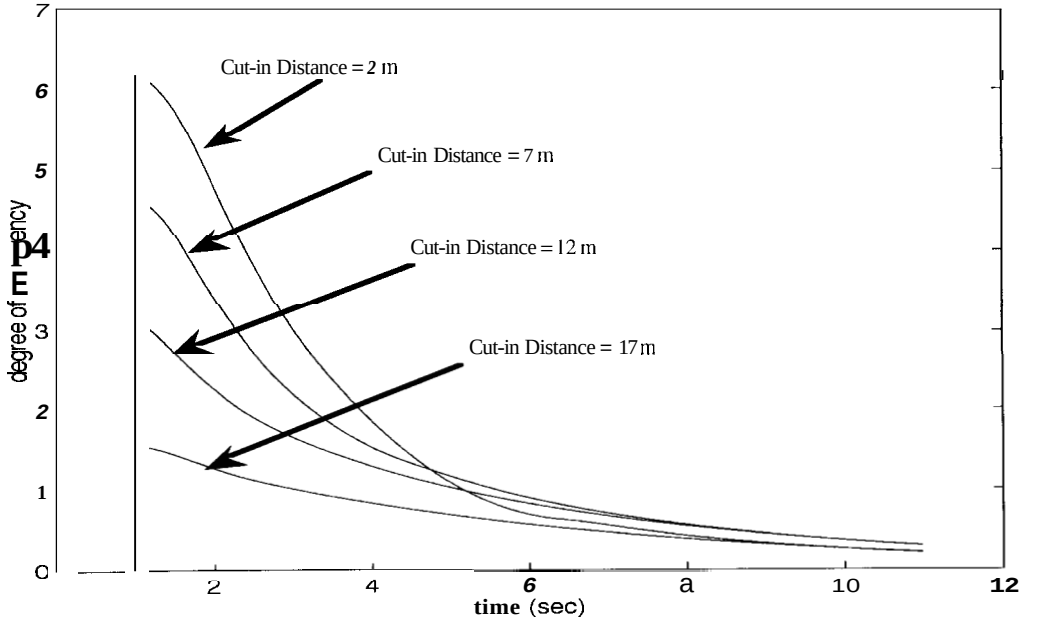

Fig. 2.3.7: Degree of Emergency in the Case of a Cut-in with CICC

If the vehicle cutting in is slower than a following one, CICC generates larger deceleration commands to a vehicle. Figures 2.3.8 (a)-(c) show the responses of a 17-meter cut-in distance with initial relative velocities of 0, -5, -10 and -12 dsec. Figure 2.3.8 (a) is of a nominal controller, Fig. 2.3.8 (b) is of a CICC, and Fig. 2.3.8 (c) is an R-Rdot diagram of both results.

While the initial, relative velocity is small, deceleration rises with a gentle slope or jerk. For instance, if the initial relative velocity is -5 dsec, the deceleration reaches 0.6 g, although its slope is still smaller than that of a nominal controller. With large initial, relative velocities such as - 10 m/sec and - 12 dsec, deceleration responses are very similar to those of a nominal controller. From the figure of R-Rdot diagrams, it is observed that the minimum inter-vehicular distances of a CICC are smaller than those of a nominal controller, and that a CICC shows some over-shoot in relative velocities. However, the differences in the minimum inter-vehicular distance become smaller as the initial, relative velocity increases because fuzzy switching generates larger deceleration commands as the degree of emergency increases.

Thus, it can be confirmed that a CICC keeps good riding comfort and achieves good collision avoidance.

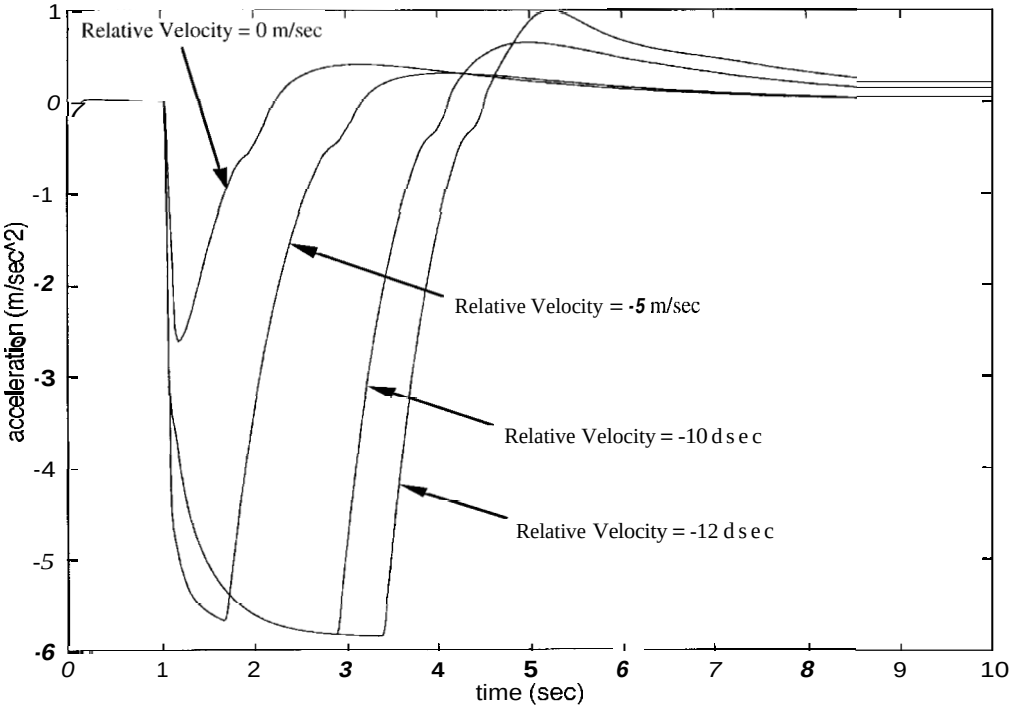

Fig. 2.3.8 (a): Cut-in with Non-zero Initial Relative Velocity (Nominal Control)

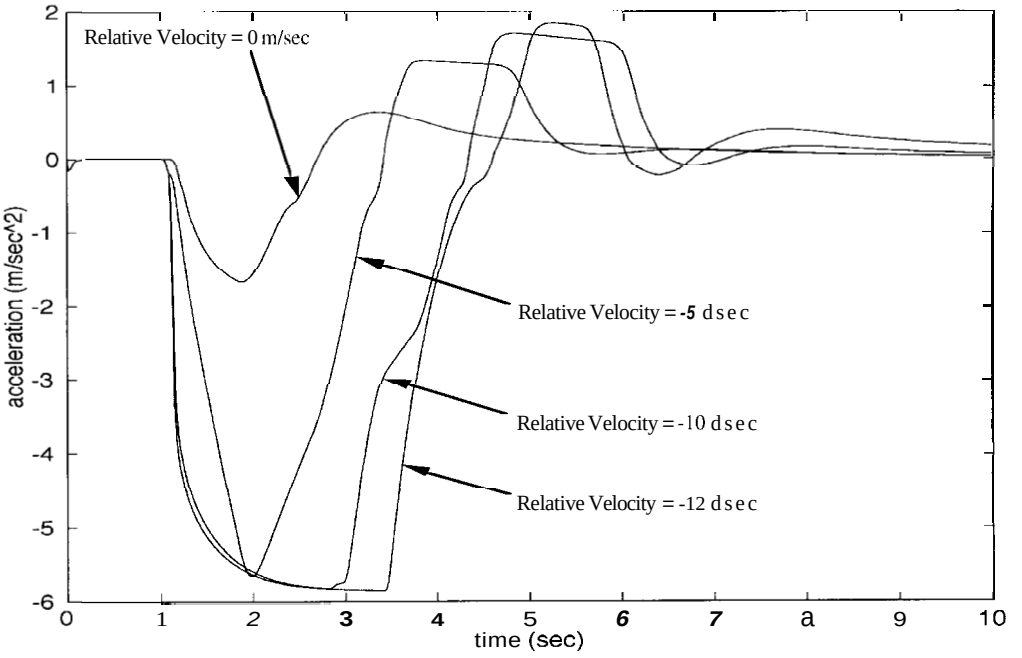

Fig. 2.3.8 (b): Cut-in with Non-zero Initial Relative Velocity (CICC)

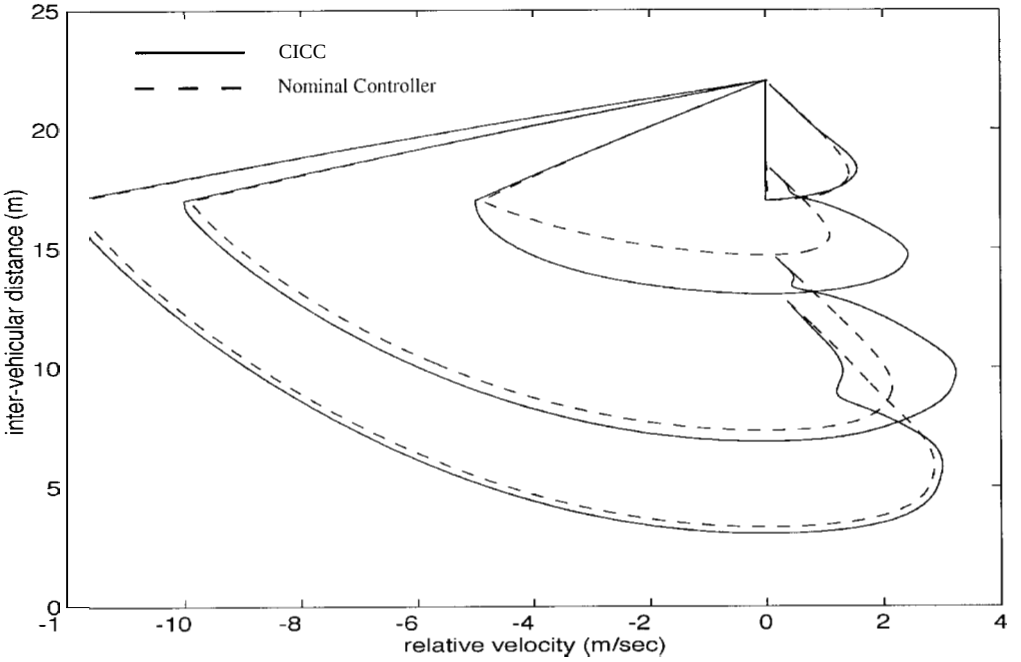

Fig. 2.3.8 (c): Cut-in with Non-zero Initial Relative Velocity (R-Rdot)

2.3.7 Effects of Acceleration Estimation

In this section, the effects of acceleration estimation (AE) will be evaluated. First, to see the performance of AE itself, open-loop simulations will be conducted. Then, to observe the effects of AE on CICC, a closed-loop simulation will be done. In the simulation, the capacity of avoiding collisions of a CICC with AE will be compared with that of a nominal controller and a CICC without AE.

2.3.7.1 Performance of Acceleration Estimation

Before being used in real-time control, AE will be evaluated in tracking performance in two situations. The situations are 1) vehicle following and 2) cut-in and cut-out of other vehicles. In both cases, sensor noise is supposed to exist in each sensor output, and the magnitudes of errors are the same as those used in the simulations in Section 2.3.4. To evaluate the performance of AE, estimated accelerations are not used in closed-loop simulations and are compared with real preceding vehicle's acceleration under noisy circumstances.

. 2.3.7.1.1 Vehicle Following

A preceding vehicle follows the velocity trajectory shown in Fig. 2.3.1, and a CICC vehicle follows it. All the control gains and parameters of the fuzzy switching are the same as those used in Section 2.3.6. Figures 2.3.9 (a) and (b) present the results of the simulation. Estimated accelerations are compared with real preceding vehicle accelerations in Fig. 2.3.9 (a), and the threshold deviations (four times as much as standard deviation) of observed errors and real errors are shown in Fig. 2.3.9 (b).

In the figures, about 0.4-seconds of delay time and about 0.2 m/sec^2 of fluctuation in estimated accelerations exist, but the estimated acceleration follows the preceding vehicle's acceleration very well throughout the maneuvering. As for estimated errors, since actual errors do not exceed threshold values, no cut-in and cut-out are detected in this maneuvering.

Thus, it can be concluded that AE works well in normal vehicle following.

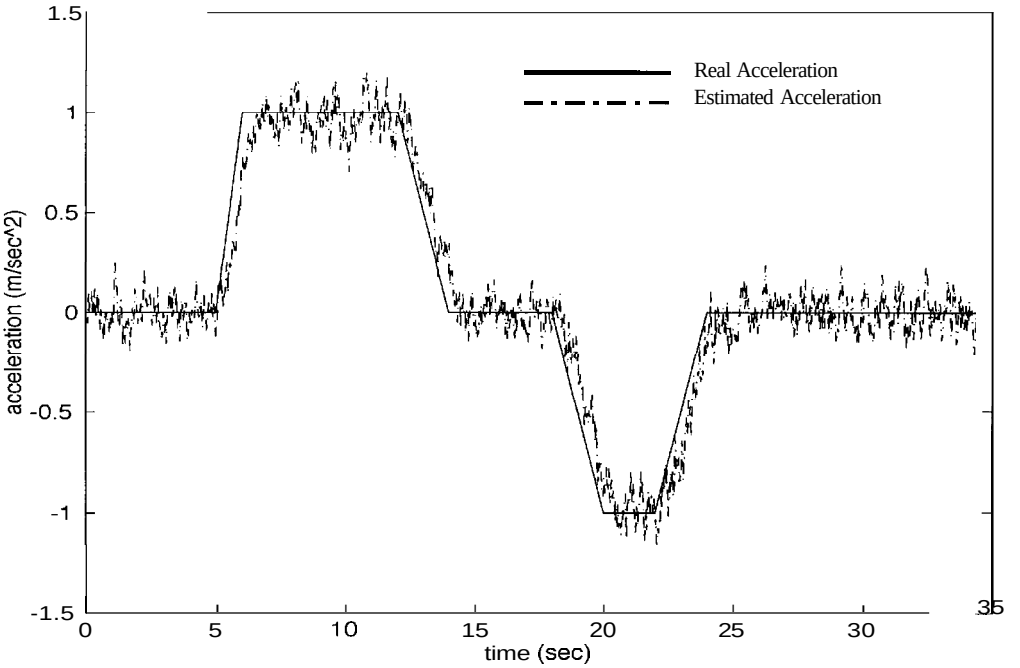

Fig. 2.3.9 (a): Real and Estimated Accelerations (Vehicle Following)

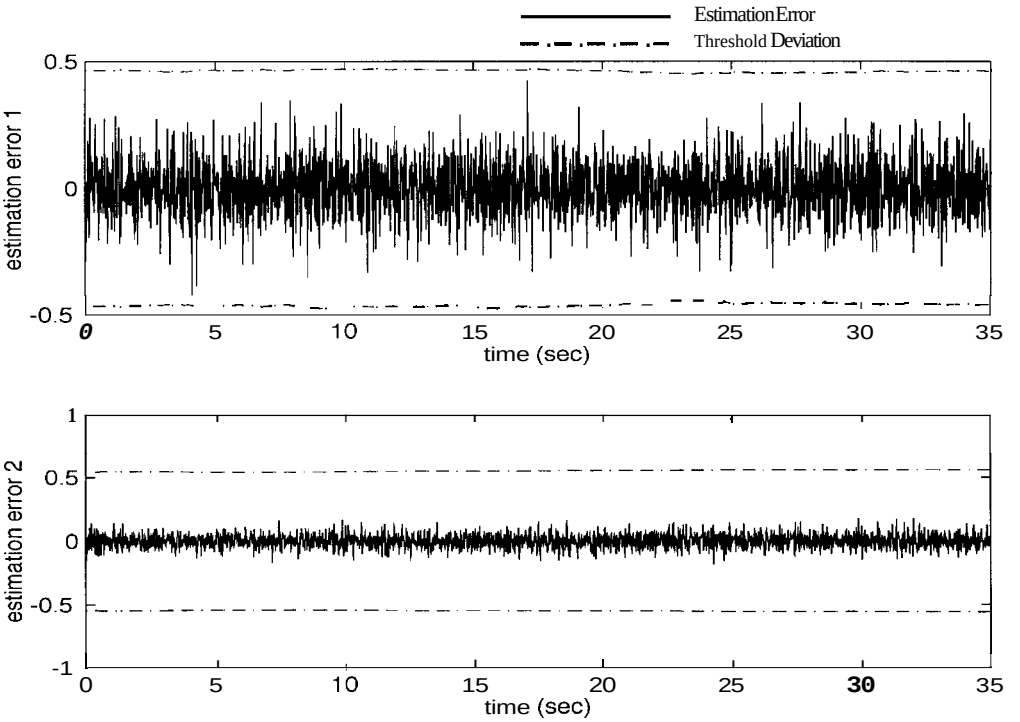

Fig. 2.3.9 (b): Estimation Errors and Threshold Deviations (Vehicle Following)

2.3.7.1.2 Cutting-in Vehicles

As previously mentioned, cut-in and cut-out seem to be major sources of disturbance in highway operations. Since AE depends on the detection filter, discontinuous inter-vehicular distance and relative velocity could cause extraordinarily large estimation errors. A cut-in detector is prepared for rejecting large disturbances due to cut-in and cut-out, and its performance will be evaluated below.

Figures 2.3.10 (a) and (b) describe responses due to a sudden cut-in. In the initial condition, a vehicle follows a preceding one with 0.7-seconds of headway time at 30 dsec. Another vehicle cuts in at a distance of 5 m closer than the desired headway distance with -12 dsec relative velocity at t = 1 sec. A cutting-in vehicle is supposed to be accelerating at a constant acceleration of 2 m/sec^2. Figure 2.3.10 (a) shows estimated acceleration and the real acceleration of the preceding vehicle, and Fig. 2.3.10 (b) describes estimation errors.

As shown in Fig. 2.3.10 (b), as soon as another vehicle appears, the cut-in detector detects cut-in by observing large fluctuations of estimated errors, and then AE is turned off for a fixed time of 0.3 seconds. As a result of that, no "spikes" or discontinuities appear in the responses of estimated acceleration (Fig. 2.3.10 (a)), and it converges at the real value within 0.9 seconds. Since the AE is turned off when cut-in is detected, it takes longer time to settle than the previous vehicle-following case.

In order to emulate cut-in, in the simulations, the outputs of inter-vehicular distance sensor and relative-velocity sensor are supposed to change their values to new ones in 0.1 seconds. It may take longer in real situations, and if another vehicle cuts in very smoothly, the cut-in detector may not detect cut-in. However, this will not be a serious problem because the primarily purpose of a cut-in detector is to avoid "spikes" in the AE. Then it is verified that with a cut-in detector, AE works well under large disturbances such as cut-in and cut-out.

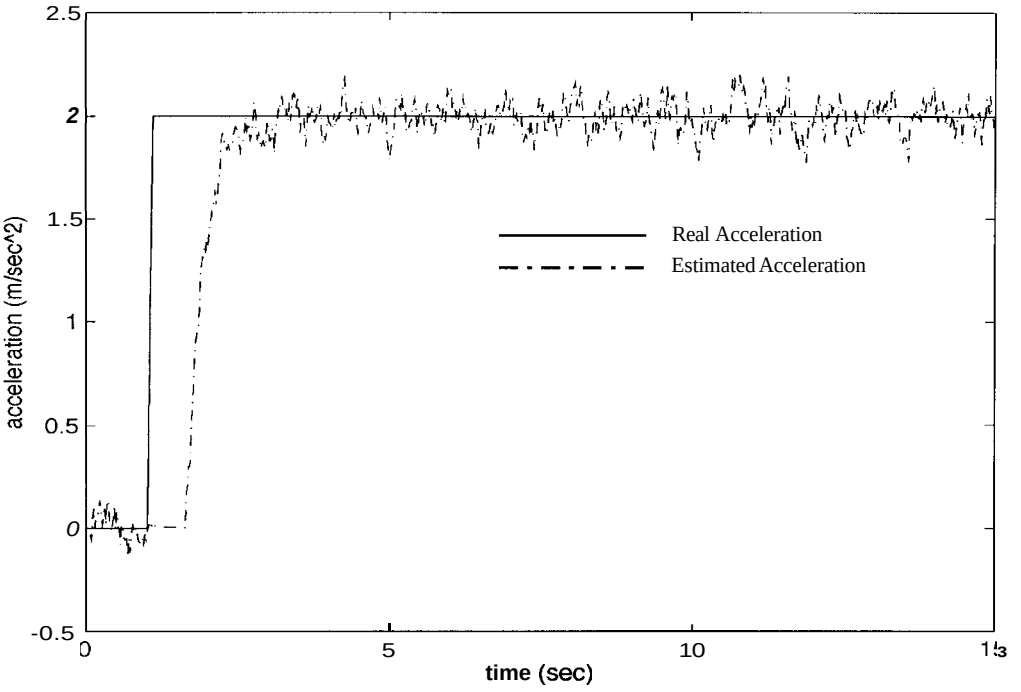

Fig. 2.3.10 (a): Real and Estimated Acceleration (Cut-in)

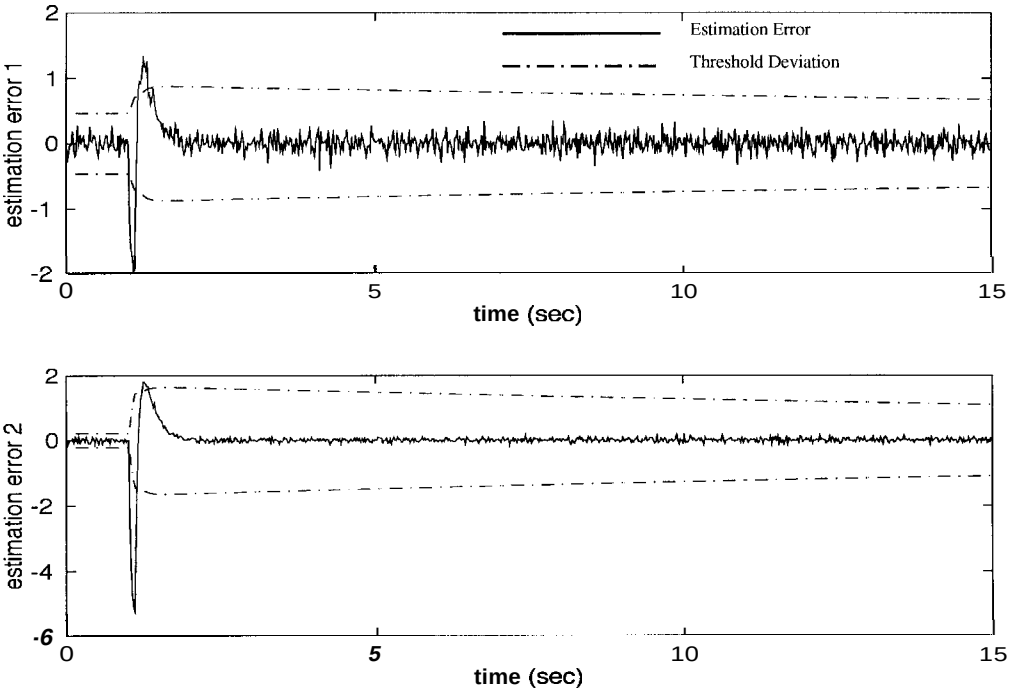

Fig. 2.3.10 (b): Estimation Errors and Threshold Deviations (Cut-in)

2.3.7.2 Estimating Acceleration in a Closed-loop Simulation

As was shown in [2, 3], the sudden braking of preceding vehicles is one of the most critical situations for collision avoidance. Although the fuzzy switching module defines a desired acceleration or deceleration based on the degree of emergency, the smoothing functions of CICC will yield delay times in sudden-brake responses, so that collisions may not be avoided effectively. The AE can improve the capacity of avoiding collisions in this case.

Then, to evaluate the performance of AE in a closed-loop, a simulation will be conducted. In the simulation, a vehicle first follows a preceding vehicle with 0.7-seconds of headway time at 30 m/sec, and then the preceding vehicle suddenly begins to decelerate at a high rate to 6 m/sec at $t = 3$ sec. The preceding-vehicle deceleration is then supposed to jump to constant values (0.6 G and 0.8 G) in 0.1 seconds. The maximum deceleration that a following vehicle can utilize is 0.6 G.

The transient responses are compared among a nominal controller, a CICC, and a CICC with AE. In the latter case, the degree of emergency is modified as described in Eq. (2.26) and applied to the fuzzy switching module.

Figures 2.3.11 (a), (b) and (c) are the results of a 0.6 G deceleration of a preceding vehicle. Figure 2.3.11 (a) presents the acceleration of vehicles under each controller. In the responses up to $t = 3$ seconds, both CICC's show smoother acceleration than does the nominal controller because of their smoothing function. When another vehicle cuts in, all the controllers begin to decelerate, but a CICC with AE does so the fastest. Figure 2.3.11 (b) shows the R-Rdot diagrams of each response. It can be seen that no collision occurs, while there is an overshoot in the responses of inter-vehicular distance with a CICC without AE. Because CICC with AE outputs the maximum deceleration command earlier than the others, relative velocity and inter-vehicular distance are smallest throughout the responses. Figure 2.3.11 (c) describes the estimated acceleration derived by CICC with **AE** (above), and the comparison of the degree of emergency in CICC with and without AE (below). **AE** successfully estimates preceding-vehicle deceleration, 0.6 G. Since the degree of emergency is modified in CICC with AE, the modified degree of emergency shows a considerably larger value than that of a CICC without AE. This makes it possible for a CICC with AE to quickly respond to preceding-vehicle braking.

Figures 2.3.12 (a), (b) and (c) are the results of a 0.8 G deceleration of a preceding vehicle. Figure 2.3.12 (a) presents the acceleration of vehicles under each controller, and the responses look similar to those of the 0.6 G deceleration, but the accelerations become the maximum deceleration earlier because a preceding vehicle decelerates at larger

decelerations. Figure 2.3.12 (b) shows R-Rdot diagrams of each response. In these cases where a CICC without AE and a nominal controller, the minimum inter-vehicular distance is below zero: this means that following vehicles collide with preceding ones. In contrast, CICC with AE successfully avoided collisions. Figure 2.3.12 (c) describes the estimated acceleration derived by CICC with AE (above), and the comparison of the degree of emergency in CICC with and without AE (below). The results show that delays exist in estimation, but the estimated acceleration follows the preceding-vehicle acceleration well. As for the degree of emergency, since CICC with AE modifies it according to estimated accelerations, the degree of emergency rises up much more steeply than that of CICC without AE.

By using AE, CICC can avoid collisions more effectively. From Figs. 2.3.12, CICC with AE performs better in both collision avoidance and riding comfort than does a nominal controller.

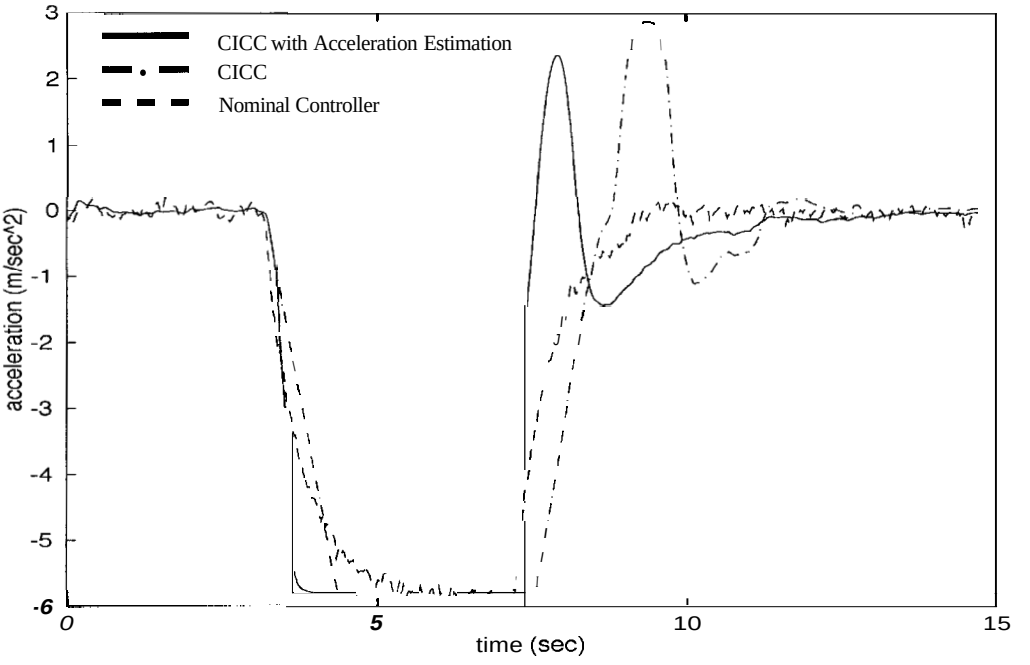

Fig. 2.3.11 (a): Sudden Braking of 0.6 G (Acceleration)

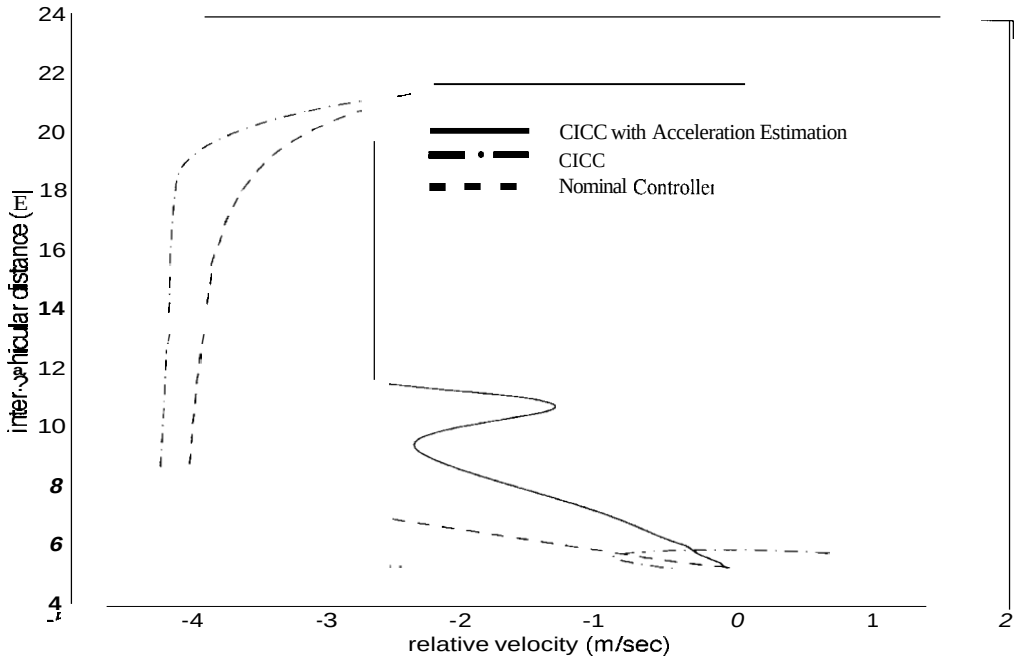

Fig. 2.3.11 (b): Sudden Braking of 0.6 G (R-Rdot Diagram)

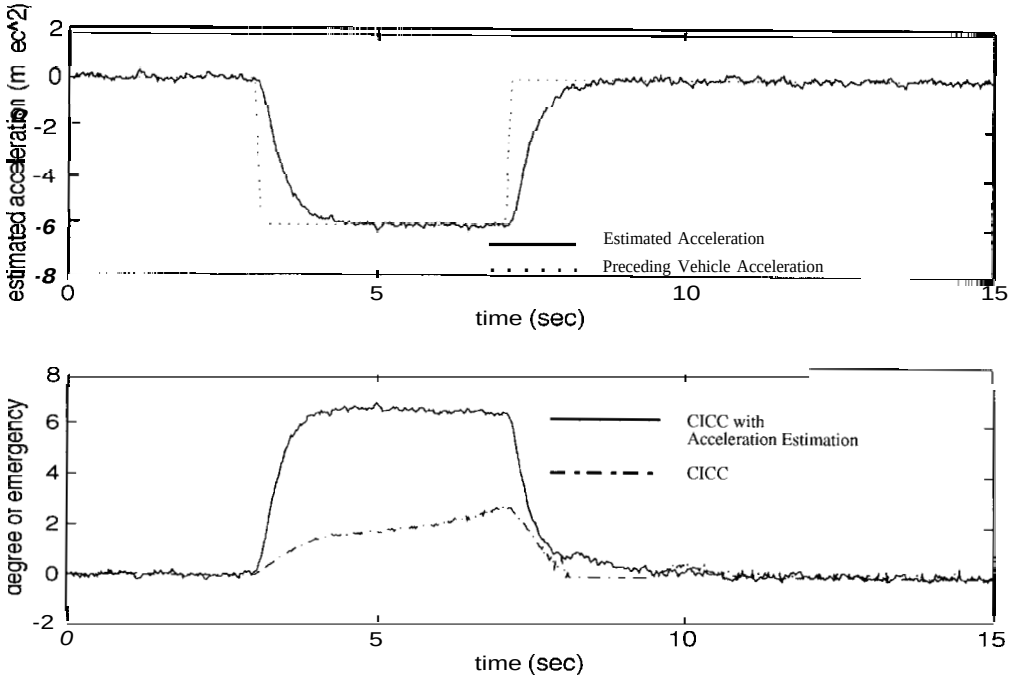

Fig. 2.3.11 (c): Sudden Braking of 0.6 G (Estimated Acceleration)

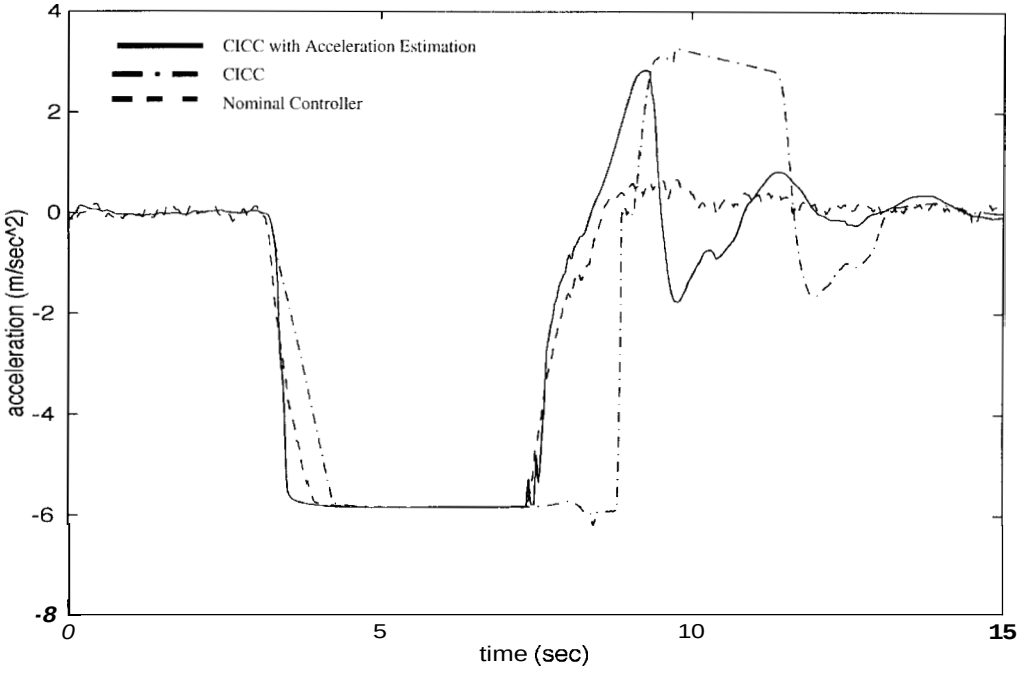

Fig. 2.3.12 (a): Sudden Braking of 0.8 G (Acceleration)

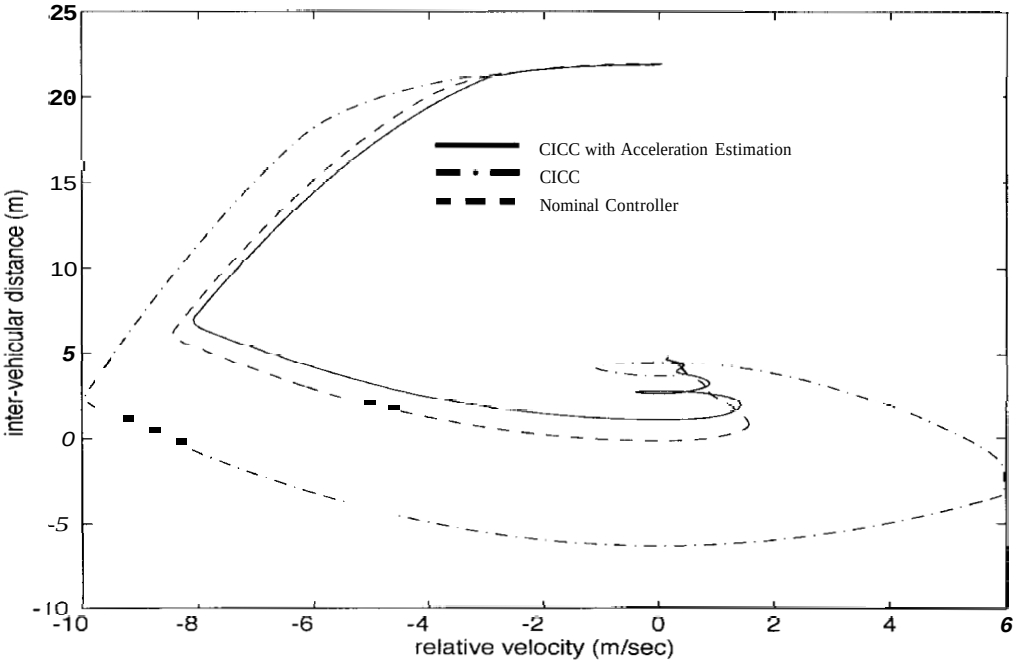

Fig. 2.3.12 (b): Sudden Braking of 0.8 G (R-Rdot Diagram)

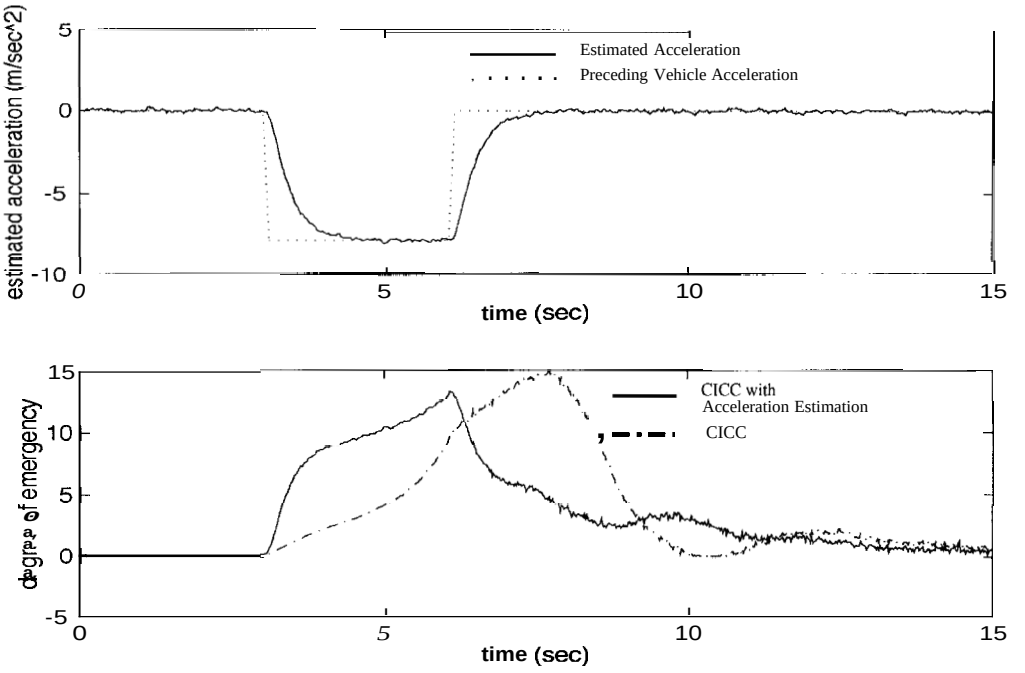

Fig. 2.3.12 (c): Sudden Braking of 0.8 G (Estimated Acceleration)

2.4 Conclusion and Future Work

Intelligent cruise control systems have become an important area of research and development, largely because their aim of these systems is to achieve greater highway capacity, while at the same time increasing the safety and comfort of drivers. As one of the systems that can fulfill these goals, CICC is examined in this report.

In Section 2.2, the concept of CICC was described, and design processes were presented in detail. CICC was equipped with several functions such as cruise control and collision avoidance. The main issue was to achieve good riding comfort and sufficient collision avoidance while assuring system stability. To do this, a fuzzy-switching logic and AE of preceding vehicles were used. The idea of detection filters was applied for AE.

In Section 2.3, the vehicle models for controllers and for non-linear simulations were presented. After investigating the effects of modeling errors on system stability, the performances of CICC were evaluated. While CICC is equipped with several control modules, the effectiveness of distancing control one in particular was verified through

non-linear simulations. These simulations consist of various situations such as vehicle following, catching up, and cutting in. The effects of sensor noise were also considered, and it was shown that CICC achieves both better riding comfort and superior capacity to avoid collisions than could a nominal headway controller.

It should be emphasized that AE improves the performance of collision avoidance. Its logic was derived based on detection filters proposed in[8]. Detection filters were used originally to detect system faults such as those of actuators and sensors by properly tuning observer gains. In this report, a detection filter was used not to detect system faults but to get information about preceding-vehicle acceleration. This was possible since detection filters, in a general sense, can extract certain lunds of information from existing systems. By applying detection filters, the effects of sensor's and actuator's noise only appear in certain direction of observer outputs. Thus, for example, to judge whether cut-in occurs or not, the error channel, in which the errors of inter-vehicular distance sensor appear, just should be observed, while neglecting the dynamic relations in systems such as the effects of current relative velocity. Then, detection filters make more intelligent controls possible by providing controllers with information that is usually concealed within the dynamics of systems.

While CICC can achieve good riding comfort and collision avoidance, it is still unclear that how it can improve the capacity of highways. Since the most important parameter to control highway capacity is desired headway time, the way to determine this is a crucial problem. To do this, it is first necessary to make clear what kinds of information are required to determine desired headway time. Second, the flow rate under real highway situations should be predicted. Some of the effects of factors for highway capacity were already evaluated in [2, 3]. However, the analyses were made only static flow rates and transient flow rates due to simple inputs such as step inputs of new headway time and moderate acceleration of preceding vehicles. To evaluate the performances of real situations on highways, time-variant, multi-lane responses in mixed flows should be considered. For this purpose, simulation tools, such as SMART PATH, must be useful; statistical approaches may be also necessary. Based on these analyses shown above, how to determine the optimal headway time should be designed.

Chapter 3
Reconfiguration of Platoons During Join and Split Maneuvers

3.1 Introduction

Within a platoon of vehicles, a communication network is established via radio (and soon, infrared) transceivers. For control and command information to flow correctly from one vehicle to the next, some sort of networking structure must be implemented. Control information refers to the data each vehicle needs to maintain its position and spacing within the platoon, while command information refers to messages exchanged between vehicles in order to negotiate higher level functions such as platoon reconfiguration. Current work has been done in the networking field by [19], which was directed towards a long term view of the PATH program. For the time being, this multilayered approach to the networking structure has not been implemented in practice. Currently, a much simpler communications architecture, which behaves like a "token bus" architecture, is implemented in our test vehicles. Up to now, only control information has been passed between vehicles. There currently exists no mechanism to direct command information from one vehicle to another.

In order to properly execute a join or split maneuver, reconfiguration of a platoon must be accomplished in real-time. Accomplishing the necessary handshaking between vehicles without disturbing the networking structure by which control information is exchanges presents a problem. Furthermore, since the possibility exists that messages may be lost (through radio interference for example), any protocol must include a procedure which provides the best possible chance of recovering from such an error.

3.2 Platoon Reconfiguration

The general idea is to create a temporary storage space where the "new" configuration of the platoon can be stored without interfering with the information necessary to send control information between vehicles. Before this temporary information can be allowed to become "active", it must be verified. Otherwise, conflicting information may exist regarding the next action to be taken by the platoon, resulting in the permanent loss of communication between vehicles. There are two communication protocols that must be dealt with. Both rely on the existance of a token architecture. The multilayered communication architecture has been developed in theory, but has not been implemented yet. In theory, it has the capability of sending messages from any vehicle to any desired destination vehicle. The simple token bus protocol currently in use lacks the capability of transmitting anything other than control information, and then only in a predetermined pattern. Eventually, the communication architecture will be switched over to the more advanced multilayered approach. Therefore, the reconfiguration protocol should be designed towards this system.

3.2.1 Proposed Implementation

The multilayered communications architecture is arranged as shown in figure 3-1,

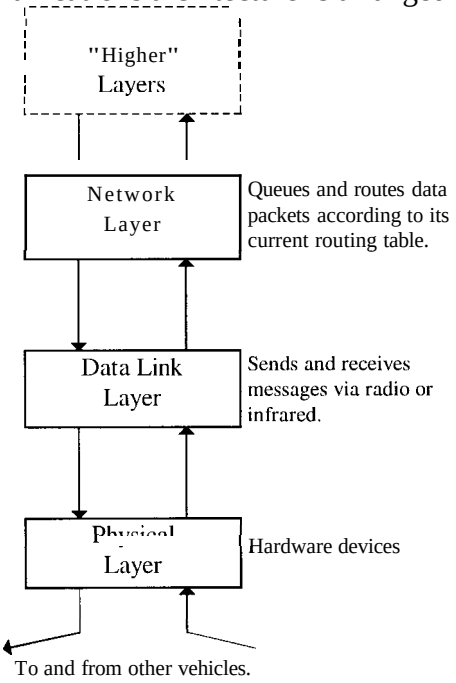

Figure 3-1 Multilayered Communications Architecture

Layers in the structure send commands to the next lower layer, and acknowledgement (ACK) or "not acknowledge" (NACK) messages or information are passed to the next higher layer. The

"higher layers" block in figure 3-1 simply points out that there are additional layers in the communication architecture that operate transparently to the network layer. **A** "routing table" or table of addresses exists in the network layer which enables a given vehicle within a platoon to keep track of the addresses of its "platoon-mates", and therefore enables it to communicate with the rest of the platoon, either through radio or infra-red links.

To effect the reconfiguration of a platoon, information regarding the location of a "new" platoon leader, and the new size of the platoon must be transmitted to each vehicle so that a new routing table can be assembled. To accomplish this, we need a new "layer" that sits on the same level as, but separate from the network layer, called the configuration manager (fig. 3-2).

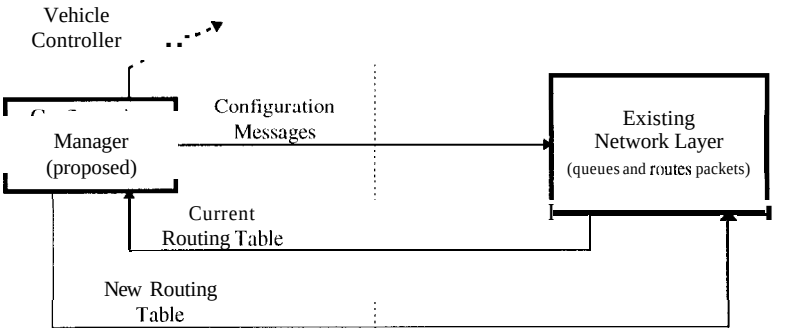

Figure 3-2 Configuration Manager

When a join or split maneuver is desired, the necessary information must be transmitted to each vehicle, and the new routing table is computed and stored in the configuration manager. This new routing table must still be verified, and during this verification process, should not interfere with the old routing table (which is still being used to transmit control information within the platoon).

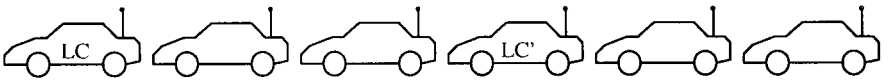

Figure 3-3 Platoon Prior to a Split

The protocol is summarized for a split maneuver as follows (LC and LC' are short for the lead car, and new lead car respectively (fig. 3-3); RT stands for the routing table). **A** more detailed flowchart describing the protocol is shown in appendix **A.**

I. LC receives a request to split message from LC', or LC decides that the platoon must be split.

II. Set up new RT's:

A. LC sends out a PREPARE to split message, which includes the position of LC', and starts a countdown of Y seconds.

B. All vehicles should be able to compute a post-split RT and place it in their configuration . manager modules.

C. If all vehicles "check in" before timer Y expires, LC issues a SPLIT in Z seconds message. . If not, ABORT.

III. Upon receiving the SPLIT message, each vehicle sends and ACK to LC and prepares to switch to the new RT in Z seconds.

IV. If all vehicles reply within (Z-factor) seconds, LC does nothing and the split occurs. If not, LC issues an ABORT message. ("factor" being the time necessary for an ABORT message to be recieved and acted upon by all vehicles)

V. Upon receiving an ABORT message, all vehicles should acknowledge the ABORT, stop the countdown, and clear the configuration manager.

3.2.2 Current Implementation

Currently, the multilayered communication architecture has not been implemented on existing vehicles. The current architecture is a very simple token bus which is designed to carry control information only. It operates as follows. Each vehicle is assigned a number which represents its position in the platoon (i.e. lead car = 1, followers = 2,...). Every 20 milliseconds, the lead car generates a token, which is essentially a message packet with special information in its header. Each follower car is programmed to receive every message from every vehicle, but to only pay attention to the messages from the lead car and the car preceding it. **If** a follower detects a broadcast from the car preceding it, it then assumes that it has the right to broadcast. Thus information flows only backwards in the platoon with no ability to send a command message from one arbitrary vehicle to another.

To enable command packets to be exchanged, four new fields must be added to the existing packet structure. One to show which vehicle originated the message, one to show which vehicle the message is intended for, and two to encode the message and any corresponding data. Since there already exists a field for the originator of the message, that leaves only three new fields to add to the packet structure.

In order to coordinate the different control laws needed to perform a join or split maneuver, the configuration layer must also be able to set certain flags which inform the control software module which control law to use. The software module that acts as the configuration manager has a program structure that follows the flowchart shown in appendix **A.**

With the current WaveLAN radios that are installed in the test vehicles, we have only one channel, which presents a problem for performing general join or split maneuvers. Two independent platoons require two radio channels to operate as truly independent entities. However, tests can be done where a free agent (single vehicle) splits off from, or joins into a platoon, in which case the second "platoon" is only a single vehicle which does not require a separate radio channel.

3.3 Future Work

Testing in the near future will involve static and dynamic tests of the split protocol for two vehicles. Once the protocol is verified for two vehicles, the tests can be expanded to four vehicle platoons. New radio technology is expected to be developed soon which would enable two or more platoons to operate simultaneously without radio interference, which should enable a "true" split maneuver to be tested.

The multilayered communication architecture will also be integrated into the test vehicles in the near future. A different block of program code must be developed for this architecture, in order to deal with, and take advantage of its increased complexity, compared to what currently exists in the test vehicles.

The join maneuver presents special problems in that "first contact" must be made between two previously independent platoons. With a split maneuver, it is comparatively easy to "break apart" an existing communication network. It is not so easy to coordinate a maneuver with (or even determine the frequency of) a platoon with which no communication previously existed. Otherwise, the join protocol should parallel the protocol for the split maneuver.

A lead vehicle control law should also be developed so that these heretofore experimental maneuvers may approach what is to be expected of them in a fully automated highway system.

Chapter 4
Longitudinal Transition Maneuvers in an Automated Highway System

4.1 Introduction

A current area of research in the field of Intelligent Vehicle Highway Systems (IVHS) is the development of a fully Automated Highway System (AHS). Under this proposed system, automated vehicles would travel in "platoons" of closely spaced vehicles in automated lanes [18]. This proposed system introduces a challenging task of how to control the vehicles such that safety and comfort are maintained.

Due to the non-linearities and parametric uncertainties of a vehicle, [15] proposed using multiple-surface sliding control techniques for performing longitudinal control of the vehicle. In this scheme, the upper surface determines a synthetic input, in the form of a desired net torque, based on the current objective of the vehicle. There are basically four longitudinal objectives of a vehicle in an AHS: lead vehicle in a platoon, following vehicle in a platoon, join a platoon or split from a platoon. The lower surface of the control structure determines either the throttle angle or brake pressure needed to achieve the desired torque.

Previous work by McMahon et. al. [15] and Gerdes and Hedrick [14] has resulted in methods to achieve the desired throttle angle and brake pressure respectively. In addition, Gerdes and Hedrick presented a switching logic to use between engine and brake control. As for the upper surface, Swaroop [17] presented a vehicle following control law which guarantees string stability within a platoon. Previous work in the area of longitudinal transition maneuvers

has resulted in both an open-loop trajectory design [16] and a closed-loop trajectory design [13]. This paper presents an upper surface control law for performing longitudinal transition maneuvers using the ideas of the closed-loop trajectory. This control law has been implemented into experimental vehicles and the results of these tests are shown.

Section 4.2 presents the relevant longitudinal dynamics of the vehicle. **A** nonlinear, uncertain state equation is derived which is later used in the development of the control law. Section 4.3 discusses the choice for the desired velocity trajectory used for the transition maneuvers. Section 4 presents the upper surface development for controlling a vehicle during a transition maneuver. Section 4.5 presents experimental results of vehicles performing transition maneuvers at normal highway speeds.

4.2 Dynamics

The relevant longitudinal dynamics needed for upper surface control law development are taken from Hedrick et. al. [9]. The equations are developed assuming there is no slip at the wheels. Figure 4.2.1 shows a bicycle model of the vehicle.

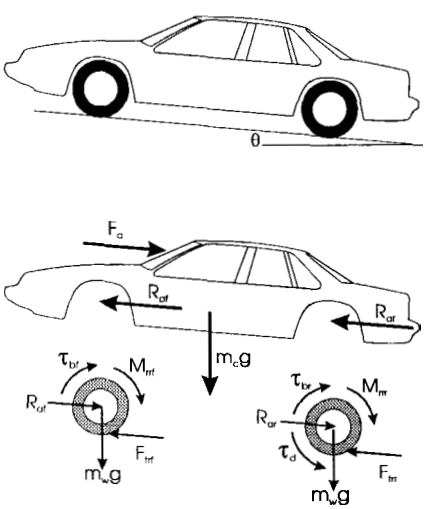

*Figure 4.2.1: Free body **Diagram** of Vehicle*

Summation of the external forces on the chassis gives:

$$R_{ar} + R_{rr} - F_a - m_c g \sin(\Theta) = m_c \dot{v} \tag{4.2.1}$$

Summation of the forces on the wheels gives:

$$-R_{af} - 2m_w g \sin(\Theta) + F_{tr,f} = 2m_w \dot{v} \tag{4.2.2}$$

$$-R_{ar} - 2m_w g \sin(\Theta) + F_{tr,r} = 2m_w \dot{v}$$

where:

R_{ar} and R_{af} are the reaction forces at the rear and front axles respectively.

$F_a = cv^2$, is the force due to aerodynamic drag.

m_c and m, are the mass of the chassis and wheel respectively.

$F_{tr,f}$ and $F_{tr,r}$ are the tractive forces at the front and rear tires respectively.

Substitution of equation 4.2.2 into 4.2.1 gives:

$$(F_{tr,f} + F_{tr,r}) - cv^2 - (m_c + 4m_w)g\sin(\Theta) = (m_c + 4m_w)\dot{v} \qquad (4.2.3)$$

Summation of moments on each wheel individually and then combining the two equations gives:

$$\tau_d - \tau_{br} - M_{rr} - (F_{tr,f} - F_{tr,r})h = I_w\dot{\omega} \qquad (4.2.4)$$

where:

τ_d and τ_{br} are the drive and total brake torque respectively.

M_{rr} is the moment due to rolling resistance.

h is the radius of the wheel.

I_w is the moment of inertia of the wheel.

Substitution of equation 4.2.4 into 4.2.3 and using the relationship between vehicle speed and wheel angular speed ($\dot{v} = h\dot{\omega}$) gives:

$$m\dot{v} = F_{net} - F_d - cv^2 \qquad (4.2.6)$$

where:

$m = m_c + 4m_w + I, /h^2$ is the total inertia of the vehicle.

$F_{net} = T_{net}/h$ is the net force generated by the engine or brakes.

$F_d = M_{rr}/h + (m_c + 4m_w)g\sin(\Theta)$ is a lumped drag force on the vehicle.

Equation 4.2.6 will be used for control law development in section 4.

4.3 Trajectory Design

A vehicle which desires to either join or split from a platoon must generate a desired velocity trajectory that will allow it to successfully perform the maneuver. This section discusses the choice of the desired trajectory used in a join maneuver. The desired trajectory for a split maneuver is determined in an similar manner. The objective of **a** join maneuver is summarized in figure 4.3.1.

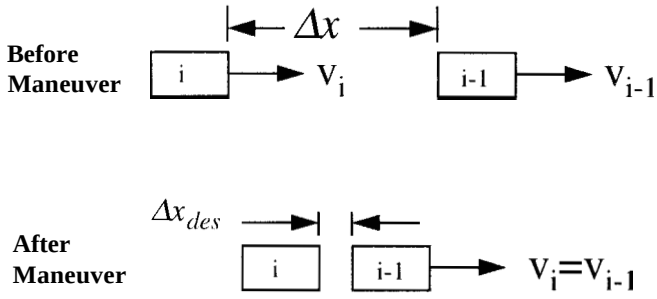

Figure 4.3.1: Objective of a Join Maneuver

The development of the optimal velocity trajectory for performing transition maneuvers has been an area of active research. [16] proposed an open-loop trajectory design. This method used the initial conditions of the maneuver (the spacing and the relative velocity between vehicle i and *i-1)* to compute a sinusoidal relative acceleration profile for vehicle *i.* Vehicle i then uses feedback of the actual spacing and velocity to ensure that the vehicle follows the desired profile. **A** potential problem with this type of trajectory design occurs if vehicle *i-1* should accelerate or decelerate while vehicle i is performing the maneuver. In order to maintain the desired relative acceleration, vehicle i may be required to accelerate or decelerate at a rate greater than it is capable of. This could lead to actuator saturation and accumulation of velocity and spacing error in the control law.

A closed-loop trajectory design was proposed by [13] which updates the velocity profile throughout the maneuver based on the current state of the system (the spacing and velocity of vehicle *i-1*). This trajectory design is the basis for the one used in this investigation, therefore, it will be described briefly.

Keeping in mind the objective of a join maneuver (figure 4.3.1), the desired velocity can be determined from the basic kinematics equation:

$$v_f^2 = v_o^2 + 2as \qquad (4.3.1)$$

where:

$v_f = v_{i-1}$, is the desired final velocity.

$v_o = v_{i,des}$, is the desired initial velocity of vehicle i.

$a = -a_{com}$, is a chosen comfortable deceleration rate.

$s = s_{i-1} + (\Delta x - \Delta x_{des})$, the distance vehicle i must travel to join vehicle *i-1*.

The approximate duration of the maneuver is $t = (v_0 - v_f)/a_{com}$. The distance vehicle *i-1* will travel in this time is $s_{i-1} = v_{i-1} \cdot t$, assuming a relatively constant v_{i-1}. By making the appropriate substitutions, equation 4.3.1 can be solved to obtain the desired velocity.

$$v_{i,des} = v_{i-1} + \sqrt{2a_{com}(\Delta x - \Delta x_{des})} \qquad (4.3.2)$$

When $\Delta x - \Delta x_{des} \le \Delta x_{switch}$, which must be positive, the control law will switch from a joining law to a follower law. Therefore, $\Delta x - \Delta x_{des}$ will never become less than 0. Equation 4.3.2 indicates that when Δx is large, the desired relative velocity can also become quite large, which decreases safety and may violate maximum velocity constraints for the highway. In order to avoid this, a limit can be placed on the relative velocity ($\Delta v_{\max}$). Therefore, the desired velocity is:

$$v_{i,des} = \min \begin{Bmatrix} v_{i-1} + \sqrt{2a_{com}(\Delta x - \Delta x_{des})} & (3.3a) \\ v_{i-1} + \Delta v_{\max} & (3.3b) \end{Bmatrix}$$

This equation can also be written as:

$$-\dot{e} = \min \begin{Bmatrix} \sqrt{2a_{com}e} & (3.4a) \\ \Delta v_{\max} & (3.4b) \end{Bmatrix}$$

where:

$e = x_{i-1} - x_i - \Delta x_{des}$, is the spacing error.

$\dot{e} = \dot{x}_{i-1} - \dot{x}_{i,des}$, is the velocity error.

The graphical representation of the desired relative velocity ($\dot{e}$) with respect to the spacing *(e)* is shown in figure 4.3.2. The dashed line is equation 4.3.4*a* plotted for all values of *e*. The solid line is the desired relative velocity when including the limit on the $\dot{e}$ (equ. 4.3.4*b*). Although this limit in the relative velocity may increase the safety of the maneuver, it will also increase the duration.

Frankel et. al. (1994) presented a trajectory design consisting of multiple stages that would optimize time and safety. The final stage is given by equation 4.3.4. The first stage is used to increase the relative velocity while maintaining a safety constraint when Δx is large. The goal of the safety constraint is to limit the relative impact velocity of the vehicles under the worst case situation, which would be if vehicle *i-1* applied maximum braking during the maneuver. The desired velocity under this safety constraint can be determined in a similar

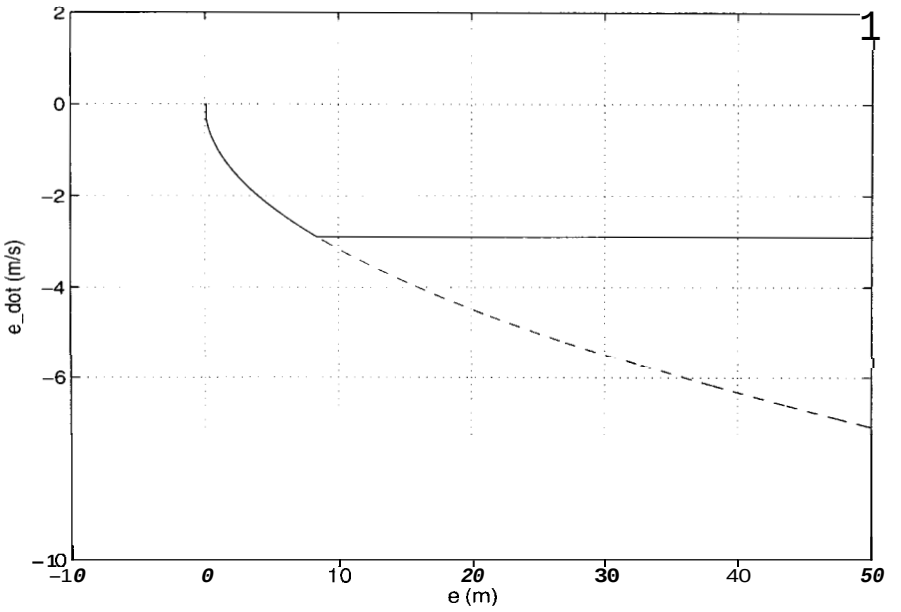

Figure 4.3.2: Desired Relative Velocity for Join Maneuver (note that $e<0$ indicates $v_i > v_{i-1}$)

manner as before, starting with equation 4.3.1.

$$v_f^2 = v_o^2 + 2as$$

where:

$v_f = v_{safe}$, is the relative velocity limit at impact.

$v_o = v_{i,des}$, is the desired initial velocity of vehicle *i*.

$a = -a_{max}$, is the maximum deceleration (note that this approach assumes similar braking capabilities between vehicle *i* and *i-1)*.

$s = s_{i-1} + \Delta x$, the distance vehicle *i* will travel before contacting vehicle *i-1*. If v_{safe} is set to $\Delta v_{\max}$, then during this stage of the maneuver, Δx is large enough such that if vehicle *i-1* applies maximum braking, it will come to a stop before being hit by vehicle *i*. Therefore, the distance vehicle *i-1* will travel is $s_{i-1} = v_{i-1}^2/(2a_{\max})$. Making the appropriate substitutions, the desired velocity is obtained:

$$v_{i,des} = \sqrt{v_{i-1}^2 + v_{safe}^2 + 2a_{max}\Delta x} \qquad (4.3.5)$$

The complete desired velocity profile is shown in figure 4.3.3. The dashed line is the desired relative velocity during the first stage, which is given by equation 4.3.5. When $-e$ reaches Δv_{max}, the desired velocity switches to the second stage of the maneuver which is given by equation 4.3.3 (solid line if fig. 4.3.3).

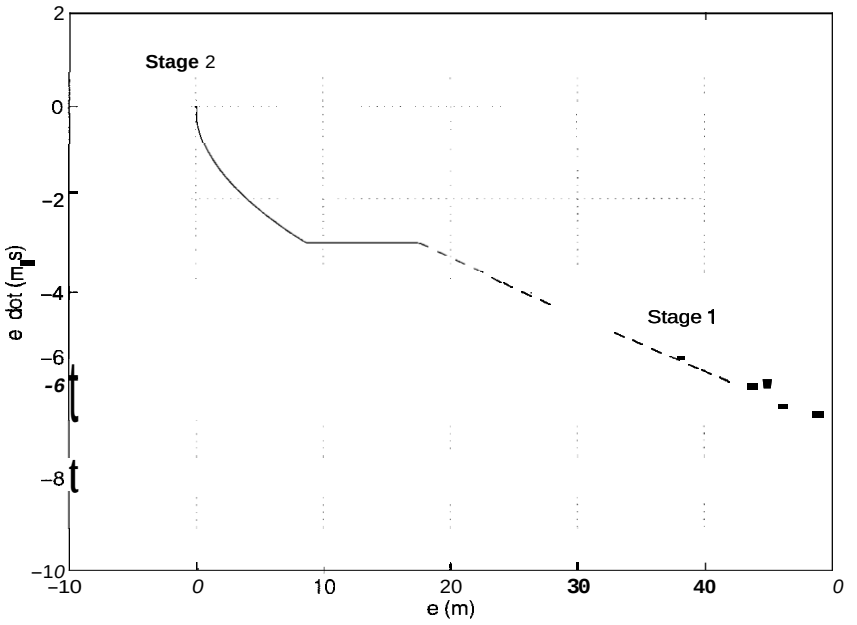

Figure 4.3.3: Desired Relative Velocityfor Join Maneuver Incorporating Safety Criteria

At this point, it is apparent that there are several options for choosing a desired velocity trajectory. The choice depends on the requirements of the system. For simplicity and safety, it is easiest to choose equation 4.3.4. This is the trajectory that was used in the experiments which are presented in section 4.5. However, if it is desired to optimize the time of the maneuver, then vehicle *i* should use the multiple stages of the maneuver as shown in figure 4.3.3. Since this maneuver allows for higher relative speeds when at large distances, the duration of the maneuver is decreased.

The desired velocity trajectory for a split maneuver is obtained in a similar manner as equation 4.3.2. As with the join maneuver, a limit is placed on the relative velocity. The resulting desired velocity is given by:

$$v_{i.des} = \max \begin{Bmatrix} v_{i-1} - \sqrt{2a_{com}(\Delta x - \Delta x_{des})} \\ v_{i-1} - \Delta v_{\max} \end{Bmatrix} \qquad \begin{matrix} (3.6a) \\ (3.6b) \end{matrix}$$

4.4 Control Development

After deterring the desired velocity trajectory, the control objective is to simply ensure that the vehicle follows the desired velocity. The control development is very similar for both a join and split maneuver. Therefore, as in section 4.3, only the development for the join

maneuver will be presented. Section 4.3 presented a trajectory design for a join maneuver that consisted of two stages. The control law used throughout the maneuver is the same, even when the equation determining the desired velocity changes. In this section, the control law development is shown using only the desired velocity given by equation 4.3.3a, since this is the final stage of the maneuver and most critical in terms of safety since Δx is approaching Δx_{des}.

A sliding control approach has been chosen due to its robustness features to parametric uncertainties. The vehicle model contains uncertainties in the parameters of the mass (m), the drag force (F_d) and the air resistance coefficient (c). In addition, by the choice of the desired velocity trajectory, a surface has already been defined as:

$$S = v_i - v_{i,des} = v_i - v_{i-1} - \sqrt{2a_{com}(\Delta x - \Delta x_{des})} \qquad (4.4.1)$$

or

$$S = -(\dot{e} + \sqrt{2ae}) \qquad (4.4.2)$$

where:

$e = x_{i-1} - x_i - \Delta x_{des}$, is the spacing error.

$\dot{e} = \dot{x}_{i-1} - \mathrm{X},,$ is the velocity error.

Figure 4.4.1(a) shows the S=O surface, as defined above, in the phase plane of the system. The phase

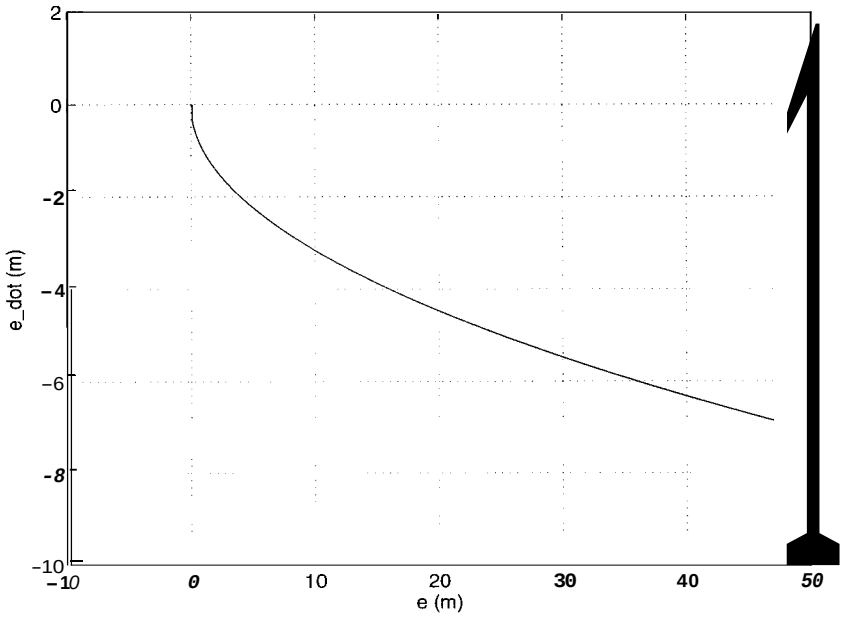

Figure 4.4.1(a): Phase Plane with the Surface S=0.

plane gives some physical insight to the problem. The origin represents vehicle *i* following vehicle *i-1* at the desired spacing and the same velocity. Clearly, one of the main objectives is to prevent the trajectory of the vehicle from entering the left hand plane, since this indicates vehicle *i* is closer than the desired spacing to vehicle *i-1*. Small overshoot into the left hand plane may be acceptable, and in reality is difficult to avoid for all situations. However, if the vehicle's trajectory should enter the left hand plane by Δx_{des} or more, the vehicles would make contact. The initial conditions of a join maneuver normally put the vehicle's position on the positive e axis in figure 4.3.2. This corresponds to an initial spacing that is greater than desired and a velocity of vehicle i that is equal to vehicle *i-1*'s. However, it is not necessary for the initial velocities to be the same. The control objective is to drive the system trajectory to the **S=O** surface and then track the surface to the origin. When the spacing error (e) gets close to 0, the objective of the vehicle will change from joining the platoon, to becoming a follower in the platoon. Therefore, the control structure of the upper surface will change from the "join" law to a "follower" law.

In order to drive the system to the desired surface, the input must be chosen such that $S\dot{S} < 0$ when not on the surface. However, choosing the input in this manner leads to chatter about the surface. Therefore, the input will instead be chosen such that $S\dot{S} < 0$ outside of a boundary layer, Φ, around the surface. Although the relaxation of this condition will reduce the tracking performance, it will also eliminate actuation chatter. In order to find the necessary input, the derivative of **S** is taken with respect to time:

$$S = \dot{v}_i - \dot{v}_{i,des} \tag{4.4.3}$$

where:

$$\dot{v}_{i,des} = \dot{v}_{i-1} + a_{com}\dot{e}/\sqrt{2a_{com}e}$$

It should be noted that when vehicle *i-1* is properly tracking the desired velocity, then $\mathbf{e} \approx -\sqrt{2a_{com}e}$. Therefore, the desired acceleration is $\dot{v}_{i,des} \approx \dot{v}_{i-1} - a_{com}$. Substituting equation 4.2.6 into 4.4.3 gives:

$$\dot{S} = \frac{F_{net} - F_d - cv^2}{m} - \dot{v}_{des} \tag{4.4.4}$$

In order to guarantee that $S\dot{S} < 0$ outside of the boundary layer, Φ, $\dot{S}$ is set equal to $-kS/\Phi$ and then equation 4.4.4 is solved for the synthetic input, F_{net}. This gives:

$$F_{net} = \hat{m}(\dot{v}_{i,des} - kS/\Phi) + \hat{F}_d + \hat{c}v^2 \tag{4.4.5}$$

where:

$\hat{m} = 214.48$ **kg.,** is the modeled mass of the car.

$\hat{F}_d = 220\,N$, is the modeled drag force when on a flat road.

$\hat{c} = 0.5$, is the modeled coefficient of aerodynamic drag.

The two remaining steps in the design of the control law are to choose values for the boundary layer, Φ, and for the surface gain, k. In order to understand how Φ is to be chosen, one must first understand what it represents. Figure 4.4.1(b) shows the **S=O** surface in the phase plane with a boundary layer represented by the dashed lines.

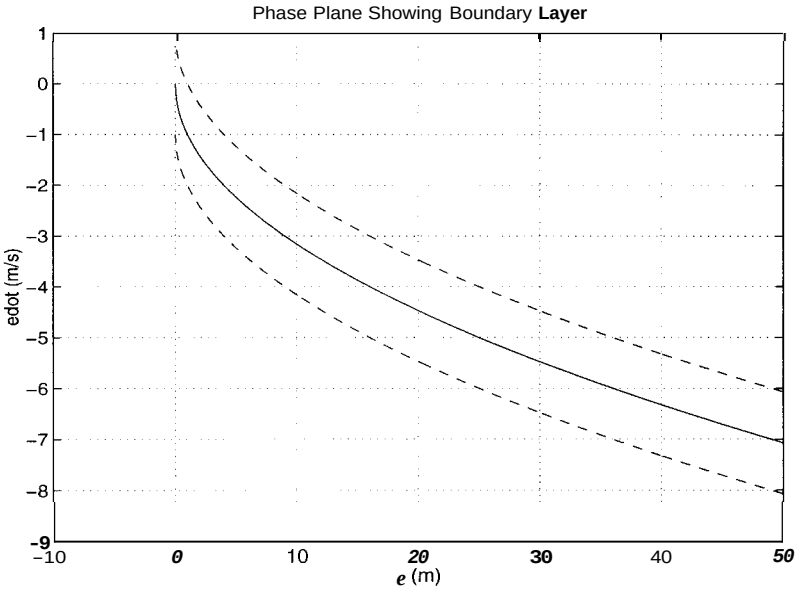

Figure 4.4.1(b): Phase Plane with S=O Surface and Boundary Layer

In this figure, Φ has been set to 1.0 m/s. Φ corresponds to an error between the desired velocity and the actual velocity of the joining vehicle. Therefore, Φ is the vertical distance from the solid line to either dashed line. With the control law shown in equation 4.4.5, $S\dot{S}$ is only guaranteed to be negative outside of the boundary layer. Therefore, once the system trajectory has entered the boundary layer, there is no guarantee that the control law will continue to drive the system to the S=O surface.

In order to choose a value for Φ, the effect of the boundary layer on the performance of the maneuver must be investigated. The velocity error becomes critical as the spacing error approaches Δx_{switch}, since this is when the switch is made to the follower control law. A velocity error at this point could cause overshoot in the spacing error. Figure 4.4.1(b) helps illustrate this point. Since the control law has been chosen such that the velocity is only guaranteed to be within the boundary layer, which is between the dashed lines, the thickness of

this layer is important. The effect of the boundary layer is that there may be an initial velocity error when the vehicle makes the transition from the join control law to the follower control law. To determine what initial velocity error is acceptable, the error dynamics of a platoon of vehicles must be examined. The follower control law which guarantees string stability within a platoon has been shown by [17] to have the same form as equation 4.4.5 with $\dot{v}_{i,des}$ chosen to be:

$$\dot{v}_{i,des} = \frac{1}{1+q_3}(\dot{v}_{i-1} + q_3\dot{v}_1 - (q_1+\lambda)\dot{\varepsilon}_i - q_1\lambda\varepsilon_i - (q_4+\lambda q_3)\cdot(v_i - v_1) - \lambda q_4(x_i - x_1 + \sum_{j=1}^{i} L_j)) \quad (4.4.6)$$

where:

x_1, v_1, and $\dot{v}_1$ are the position, velocity and acceleration of the lead vehicle.

L_j is the length of the *jth* vehicle.

q_1, q2, q_4 and λ are control gains.

The error dynamics are described by the following variables:

$$\varepsilon_i = x_i - x_{i-1} - \Delta x_{des} - L_i \quad (4.4.7a)$$

$$\varepsilon_i = v_i - v_{i-1} \quad (4.4.7b)$$

$$\ddot{\varepsilon}_i = \dot{v}_{i,des} - v_{i-1,des}\,. \quad (4.4.7c)$$

Substitution of equation 4.4.6 into 4.4.7c and taking the Laplace transform gives:

$$\varepsilon_i(s) = H_1(s)\varepsilon_{i-1}(s) + H_2(s)\varepsilon_{i,0} + H_3(s)\dot{\varepsilon}_{i,0} \quad (4.4.8)$$

where:

$$H_1(s) = \frac{s+q_1}{(1+q_3)s+(q_1+q_4)}$$

$$H_2(s) = \frac{(1+q_3)s+(q_1+q_4+\lambda(1+q_3))}{(1+q_3)s^2+(q_1+q_4+\lambda(1+q_3))s+\lambda(q_1+q_4)}$$

$$H_3(s) = \frac{1+q_3}{(1+q_3)s^2+(q_1+q_4+\lambda(1+q_3))s+\lambda(q_1+q_4)}$$

Equation 4.4.8 relates the error dynamics of the *i*th vehicle to those of the *i-1*th vehicle and the initial spacing and velocity errors of the *i*th vehicle. If vehicle *i* is performing a join maneuver, the initial spacing error, $\varepsilon_{i,0}$, will be equal to the spacing when the switch is made from the join control law to the follower control law, which will be referred to as Δx_{switch}. The initial velocity error of vehicle i will then be:

$$\dot{\varepsilon}_{i,0} = \sqrt{2a_{com}\Delta x_{switch}} \pm \Phi \quad (4.4.9)$$

It is assumed that when vehicle i is switching from a joining vehicle to a following vehicle, vehicle *i-1* is at steady state, which implies ε_{i-1}=0. The time response of the error dynamics for vehicle i can be found by taking the inverse Laplace transform of equation 4.4.8. This gives:

$$\varepsilon_i(t) = \frac{1}{a-a}(-\lambda e^{-\alpha t} + \alpha e^{-\lambda t})\varepsilon_{i,0} + \frac{I}{a-a}(-e^{-\lambda t} - e^{-\alpha t})\dot{\varepsilon}_{i,0} \qquad (4.4.10)$$

where:

$$\alpha = \frac{q_1 + q_4}{\quad} \quad]+\ \%$$

Acceptable values for the control gains have been shown to be q_1=1.0, q_2=1.5, q_3=0.5 and λ=1.0 (Swaroop, 1995). The distance at which the switch is made from join to follower control law was chosen to be Δx_{switch} = 0.1 m. Therefore, the initial spacing error ($\varepsilon_{i,0}$) in equation 4.4.10 is 0.1 m. and the initial velocity error is given by equation 4.4.9 with a_{com} = 0.5 m/s^2. Using these values the time response of equation 4.4.10 was plotted to determine acceptable values for Φ. Figure 4.4.2 shows the time response with Φ=0 and Φ=0.6.

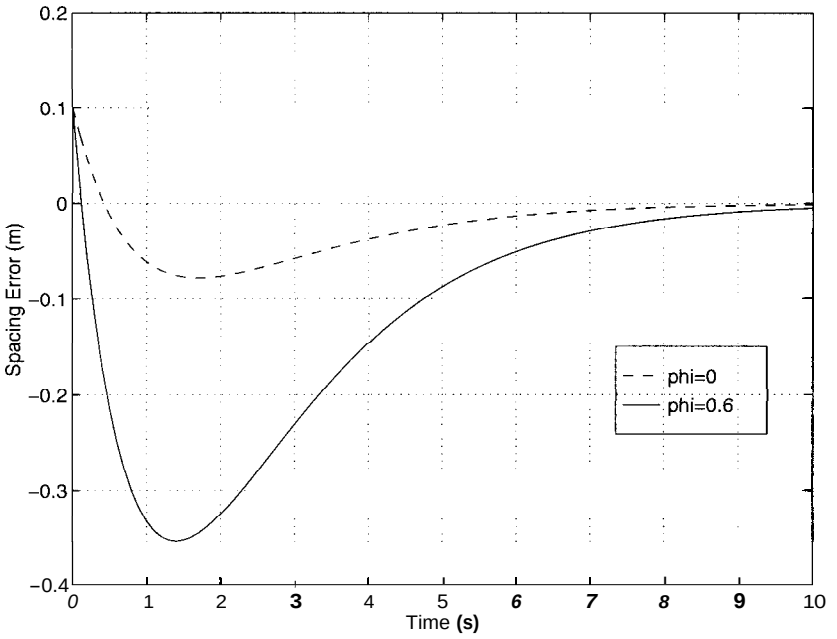

Figure 4.4.2: Response of Vehicle Under Follower Control Law to Initial Spacing ***Error***

Keep in mind that a spacing error of 0 m in the figure indicates the actual spacing is at Δx_{des}. **A** negative spacing error indicates the spacing is less than Δx_{des}. The figure shows that when Φ=0, meaning the joining vehicle was tracking the desired velocity perfectly, there is an overshoot in spacing error of less than 10 cm. The overshoot in spacing error was found to be approximately 35 cm with Φ=0.6. In the experiments presented in this paper, Δx_{des} was chosen to be 3 m, therefore, an overshoot of 35 cm was considered acceptable. The value of Φ can obviously be changed if it is desired to reduce the overshoot, especially if Δx_{des} is decreased.

The final step in the controller design is to choose the gain, ***k***, such that $S\dot{S}$ is guaranteed to be negative outside of the boundary layer even when faced with parametric uncertainties. Substituting equation 4.4.5 into 4.4.4 and then substituting equation 4.4.4 into the inequality $S\dot{S} < 0$ gives:

$$S\left[(\frac{\hat{m}}{\hat{m}} - 1)\dot{v}_{des} - \frac{hi}{\hat{m}} k \frac{S}{\Phi} + \frac{\Delta F_d}{m} + \frac{\Delta c v^2}{m}\right] < 0 \qquad (4.4.11)$$

where bounds for the uncertainties are chosen as follows:

$$\Delta F_d = \left|\hat{F}_d - F_d\right| \le \alpha = 1000N$$

$$Ac = \left|\hat{c} - c\right| \le 6 = 0.25$$

$$\beta_{min} \le \frac{\hat{M}}{M} \le \beta_{max}$$

where:

$$\beta_{min} = \hat{M}/(M + \Delta M)$$

$$\beta_{max} = \hat{M}/(M - \Delta M) \text{ with } \Delta M = 200\ kg.$$

Therefore, for the analysis, a 50% error in the air resistance coefficient has been chosen. The bound of 1000 N on the drag force corresponds to the road having an angle of about 2.5°. Obviously there are road conditions that will exceed this bound. However, choosing a higher bound will create problems for control. It is assumed that in an automated highway system there would be methods to get a reasonable estimate of F_d, since it can vary greatly on any stretch of road. These estimates could come from accelerometer measurements or roadside communication. The bound on the mass of 200 kg corresponds to an estimate of the varying loads on the vehicle due to varying number of passengers and cargo.

In order to guaranteed that $S\dot{S} < 0$, the worst case situation is considered and then k is found to be:

$$k > \frac{1}{\beta_{min}}\left[\frac{\alpha}{M_{min}} + \frac{\delta}{M_{min}} v^2 + (\beta_{max} - 1)\left|\dot{v}_{des}\right|\right] \qquad (4.4.12)$$

Therefore, the control law described by equation 4.4.5, with k chosen to satisfy equation 4.4.12, will guarantee that $\mathbf{S}\dot{\mathbf{S}} < 0$ outside of the boundary layer, Φ, which was chosen to be 0.6. So the system trajectory will be driven to within the boundary layer and then follow the surface to the origin of the phase plane. At this point the follower control law will take over to regulate the system about the origin.

4.5 Results

Experiments were performed using two Ford Lincoln Towncars equipped with both throttle and brake actuators. The range limitation of the radar units used to determine spacing is 30 m. Figure 4.5.1 show the results of a join maneuver which started with a spacing of 25 m. and had a final desired spacing of 3 m. The desired velocity profile for the maneuver is given by equation 3.3 with $\Delta v_{\max} = 2\ d\ s$. The lead vehicle maintained a constant velocity of 24.5 m/s throughout the maneuver. The join maneuver was initiated at 7 seconds, at which point the computer starts computing a desired velocity, which is shown by the dashed line. The desired velocity shown comes from equation 3.3a. This shows that the computer continually computes the desired velocity given by equation 3.3a, even when the velocity is limited such that **Av** remains at 2 m/s. After the maneuver was initiated, the vehicle accelerates until it reaches Δv_{max}. It then maintains this relative velocity until it reaches the desired velocity curve. The plot of the

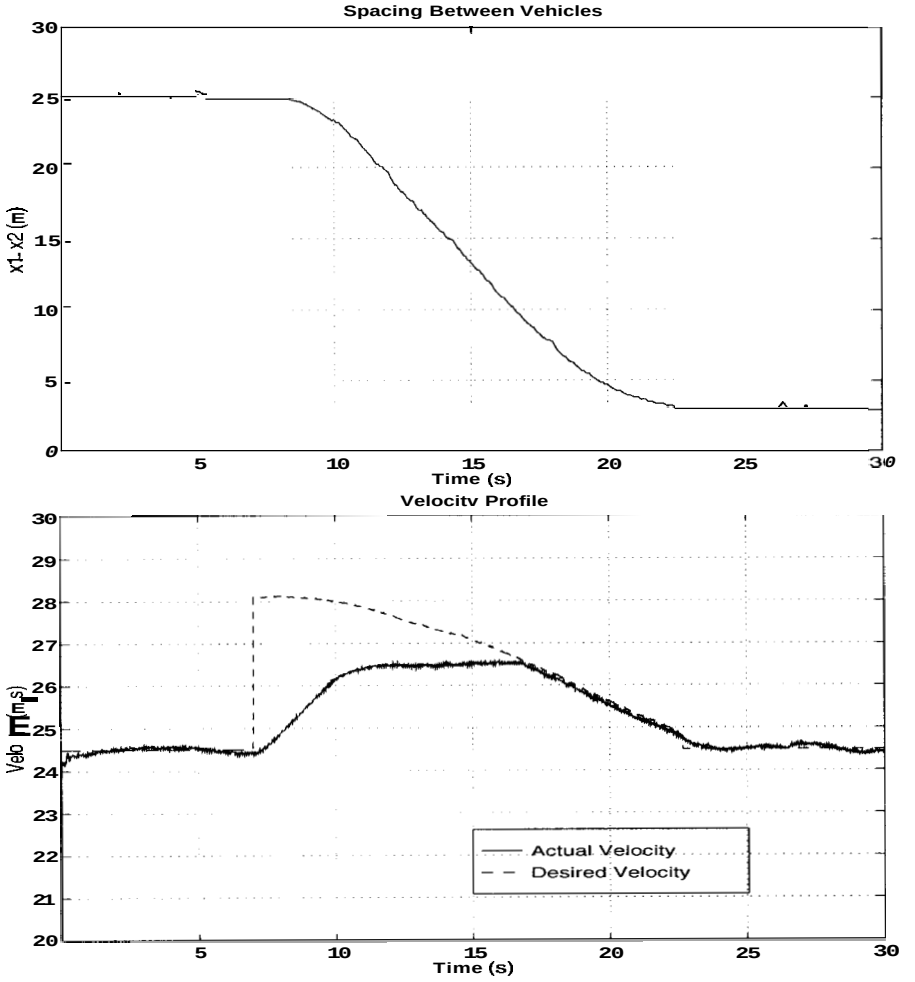

*Figure 4.5.1: Results of **Join** Maneuver Test*

spacing between the vehicles shows that the vehicle successfully decreased the spacing from 25 m to 3 m, at which point the joining vehicle has reached the same speed as the lead vehicle. It then maintains the 3 m spacing between it and the lead vehicle using the follower control law.

Figure 4.5.2 shows the results of a split maneuver which began at 4 m and ended with a spacing of 25 m. The lead vehicle maintained a constant velocity of 24.5 m/s. Like the join maneuver, the maneuver was begun at 7 seconds and Δv_{max} was set to 2 m/s. Therefore, the vehicle first decelerates until it reaches the maximum relative velocity. It then maintains this velocity until it reaches the desired velocity curve (dashed line). The figure of the spacing shows that the vehicle successfully increased its spacing from 4 m to 25 m.

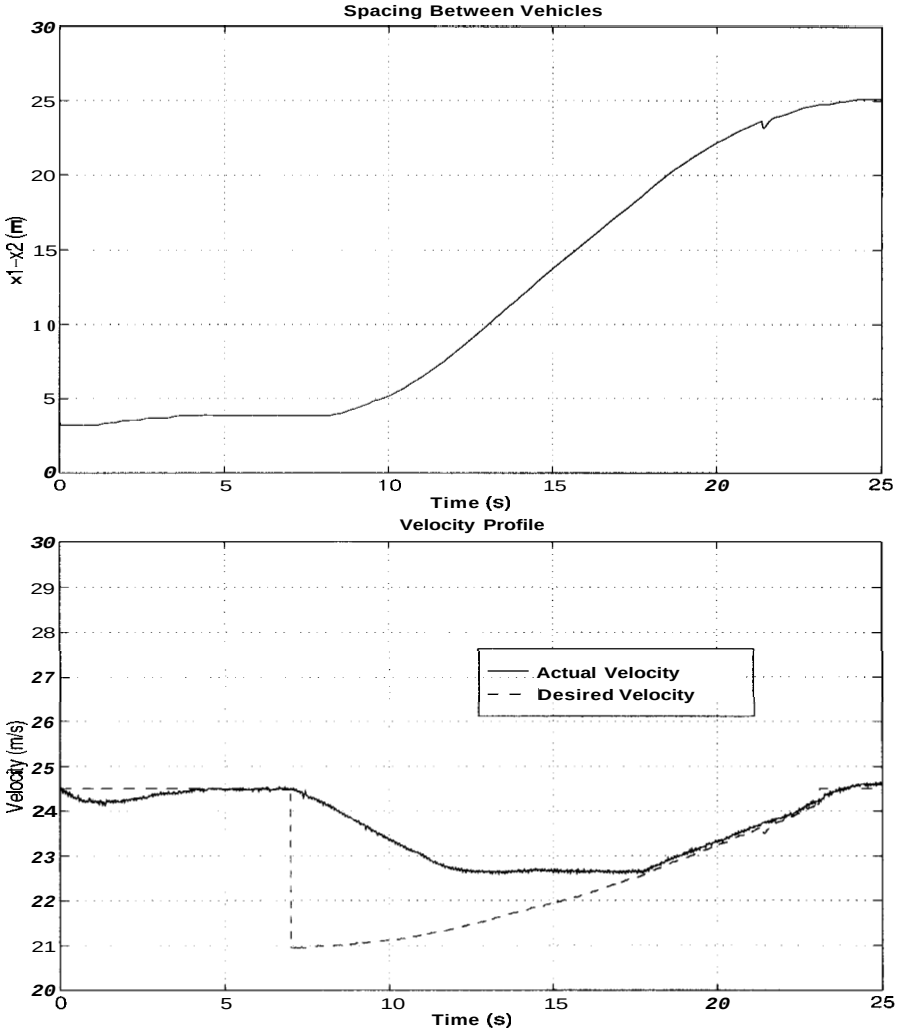

Figure 4.5.2: Results of Split Maneuver Test

Chapter 5 Conclusion

As an important aspect of PATH, longitudinal control has emphasized the concept of vehicle following control and has been studied in the past years. CICC is chosen as an Intelligent Cruise Control to increase not only the highway capacity but also the safety and comfort of drivers. The method requires an automatic throttle and brake control and simple infrastructure-vehicle communication and it is designed to let a vehicle operate under a conventional cruise control system in the absence of traffic around the controlled vehicle but will work as a distancing control system when other vehicles are within the range of its sensors.

In this report, the concept of CICC was described, and design processes were presented in detail. CICC was equipped with several functions such as cruise control and collision avoidance. The main issue was to achieve good riding comfort and sufficient collision avoidance while assuring system stability. To do this, a fuzzy-switching logic and AE of preceding vehicles were used. The idea of detection filters was applied for AE. Also, the vehicle models for controllers and for non-linear simulations were presented. After investigating the effects of modeling errors on system stability, the performances of CICC were evaluated. While CICC is equipped with several control modules, the effectiveness of distancing control one in particular was verified through non-linear simulations. These simulations consist of various situations such as vehicle following, catching up, and cutting in. The effects of sensor noise were also considered, and it was shown that CICC achieves both better riding comfort and superior capacity to avoid collisions than could a nominal headway controller.

Vehicles within a platoon depend on a communication network to provide the information necessary to maintain stable control at such close inter-vehicular spacing. To

join two platoons together, or to split one platoon apart "on the fly" requires that this communication network be disturbed. A protocol must be developed for each of these maneuvers such that the control information being passed through this network remains as unperturbed as possible during the reconfiguration of the platoon networking structure.

A protocol for a platoon split maneuver has been developed in chapter 3, and is being readied for testing. It was designed with a multilayered communications architecture in mind (which currently exists only in theory, but is to be implemented in the near future). In order to implement the protocol within the currently existing software in the test vehicles, no fundamental changes in the protocol were necessary. However, certain abilities of the multilayered architecture had to be added into the existing software. As this work is just entering the test stage, results are not available yet.

The control structure for automated vehicles in an Automated Highway System is based on the idea of multiple-surface sliding control. The "upper" surface determines a desired net torque while the "lower" surface determines the required throttle angle or brake pressure needed to achieve the desired torque. Chapter 4 presents an upper surface control law for performing longitudinal transition maneuvers. The maneuvers use desired velocity trajectories which are based on maintaining safety and comfort throughout the maneuver. The control law chosen is a sliding controller due to the non-linearities in the dynamics and the uncertainties in the parameters. The controller was implemented into experimental vehicles and tested at highway speeds. Control laws for join maneuvers were successfully implemented enabling an experimental vehicle to go from an initial spacing of 25 m to 3 m in approximately 15 seconds. Control laws for split maneuvers were also implemented enabling an experimental vehicle to go from an initial spacing of 4 m to 25 m in approximately 15 seconds as well.

After the three year's research, the platoon maneuver for automated high way system has been studied. The theoretical analysis and the field test are used for verify the longitudinal control law and controller design for platooning and lateral control on lane following. The design and analysis of the intermediate maneuvers can be adopted to AHS applications. And the research should be keep going on further area .

Appendix：Protocol for Platoon Split Maneuver

The dotted arrow indicated a transition taken if none of the events depicted occur:

The thick gray arrows labeled with ABORT transition to the second portion of the diagram and the end point of the transition is indicated with the same type of arrow:

Before the Lead Car broadcasts its PREPARE message, it must check with a base station to request a new radio frequency/code for the "new" platoon. This new frequency should be broadcast in the PREPARE message, so that when the split occurs, a new radio link is set up immediately between the subplatoons.

Timer X: Sets how long LC will wait for ACKl's before retransmitting a PREPARE message.

Timer Y: Sets the maximum time the split maneuver will be retried without succeeding.

Timer Z: Set so that all vehicles should receive the SPLIT message. Allows sychronous switching of the routing tables

T_{factor}: Set so that an ABORT message will have time to get through before timer Z expires.

Timer W: Sets the time to retransmit for an ABORT message.

Timer V: Sets the time to retransmit for a REJOIN message.

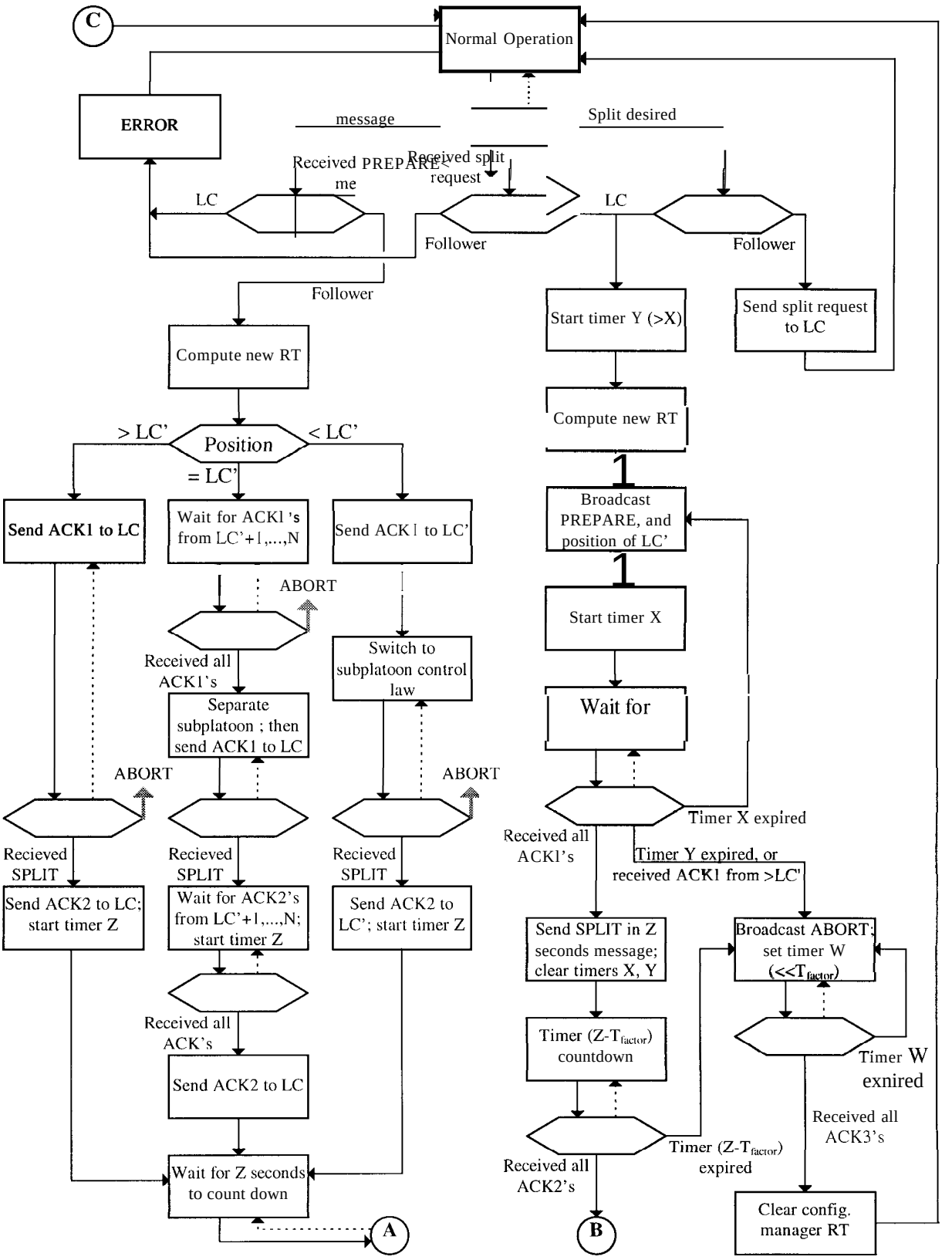
C
Normal Operation
ERROR
message
Split desired
Received PREPARE message
Received split request
LC
Follower
LC
Follower
Follower
Start timer Y (>X)
Send split request to LC
Compute new RT
Compute new RT
> LC'
Position
< LC'
= LC'
Broadcast PREPARE, and position of LC'
Send ACK1 to LC
Wait for ACK1's from LC'+1,...,N
Send ACK1 to LC'
Start timer X
ABORT
Received all ACK1's
Switch to subplatoon control law
Wait for
Separate subplatoon ; then send ACK1 to LC
ABORT
ABORT
Timer X expired
Recieved SPLIT
Recieved SPLIT
Recieved SPLIT
Received all ACK1's
Timer Y expired, or received ACK1 from >LC'
Send ACK2 to LC; start timer Z
Wait for ACK2's from LC'+1,...,N; start timer Z
Send ACK2 to LC'; start timer Z
Send SPLIT in Z seconds message; clear timers X, Y
Broadcast ABORT; set timer W (<<T_factor)
Timer (Z-T_factor) countdown
Timer W exnired
Received all ACK's
Send ACK2 to LC
Received all ACK3's
Timer (Z-T_factor) expired
Received all ACK2's
Wait for Z seconds to count down
Clear config. manager RT
A
B

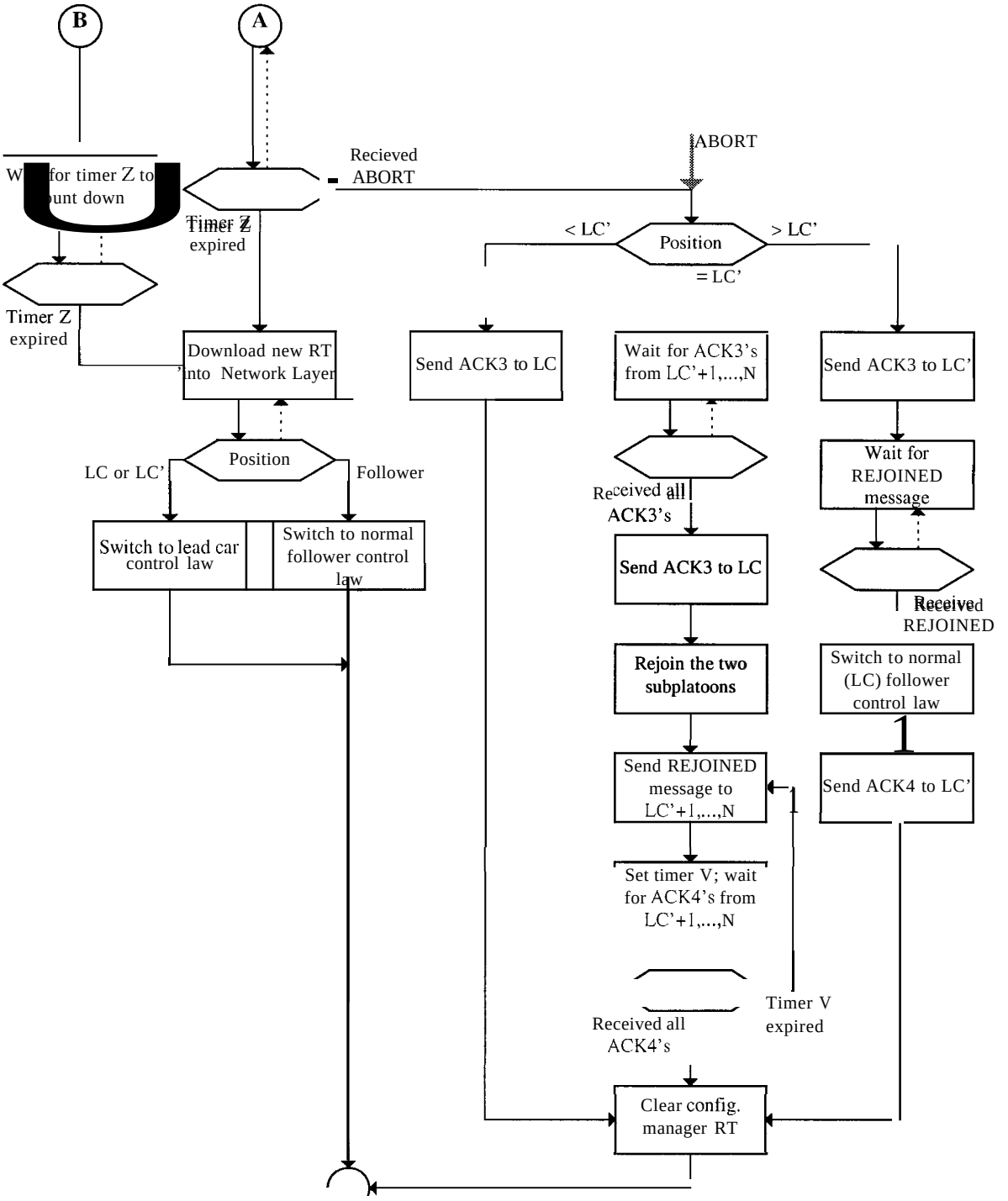
B
A
Recieved ABORT
ABORT
Timer Z expired
< LC'
Position
> LC'
= LC'
Timer Z expired
Download new RT into Network Layer
Send ACK3 to LC
Wait for ACK3's from LC'+1,...,N
Send ACK3 to LC'
LC or LC'
Position
Follower
Received all ACK3's
Wait for REJOINED message
Switch to lead car control law
Switch to normal follower control law
Send ACK3 to LC
Received REJOINED
Rejoin the two subplatoons
Switch to normal (LC) follower control law
Send REJOINED message to LC'+1,...,N
Send ACK4 to LC'
Set timer V; wait for ACK4's from LC'+1,...,N
Timer V expired
Received all ACK4's
Clear config. manager RT

Acknowledgments

The authors would like to thank the numerous individuals of the California PATH Program for their assistance in this research. This research was performed as part of the PATH program at the University of California, in cooperation with the State of California, Business, Transportation, and Housing Agency, Department of Transportation and the United States Department of Transportation, Federal Highway Administration. This work was supported in part by a National Science Foundation Graduate Research Fellowship.

Bibliography

[1] S. E. Shladover, C. A. Desoer, J. K. Hedrick, M. Tomizuka, J. Walrand, W. B. Zhang, D. McMahon, H. Peng, S. Sheikholeslam and N. McKeown, "Automatic Vehicle Control Developments in the PATH Program," IEEE Transaction on Vehicular Technology, vol. 40, 1991.

[2] Tohru Yoshioka, " Cooperative Intelligent Cruise Control System, " ME (Master of Engineering) Report, Department of Mechanical Engineering, UC. Berkeley, 1994.

[3] Hedrick, K, Varaiya, P, Pantarotto , M, Yoshioka, T, Chen , Y-H, and Connolly, T., "Integrated Maneuvering Control Design and Experiments : Phase II ", Final Report for MOU 99

[4] P. Ioannou and Z. Xu, " Throttle and Brake Control Systems for Automatic Vehicle Following," CATT Report 93-05-01, May 1993.

[5] D. E. Olson and W. L. Garrard, "Model-Follower Longitudinal Control for Automated Guideway Transit Vehicles," IEEE Transactions on Vehicular Technology, Vol. VT-28, No. 1, February 1979.

[6] P. Fancher and Z. Bareket, "Evaluation Headway Control Using Range Versus Range-Rate Relationships,"The University of Michigan Transportation Research Institute, 1993.

[7] R. N. Clark, "A Simplified Instrument Failure Detection Scheme," IEEE Transactions on Aerospace and Electronic Systems, Vol. AES-14, No. 4, July 1978.

[8] J. E. White and J. L. Speyer, " Detection Filter Design : Spectral Theory and Algorithms," IEEE Transactions on Automatic Control, Vol. AC-32, No. 7, July 1987.

[9] J. K. Hedrick, D. H. McMahon and D. Swaroop, "Vehicle Modeling and Control for Automated Highway Systems," PATH Technical Report, UCB-ITS-PRR-93-24, 1993.

[10] J. E. White and J. L. Speyer, "Detection Filter Design: Spectral Theory and Algorithms," IEEE Transactions on Automatic Control, Vol. AC-32, No. 7, July 1987.

[11] R. N. Clark, "A Simplified Instrument Failure Detection Scheme," IEEE Transactions on Aerospace and Electronic Systems, Vol. AES-14, No. 4, July 1978.

[12] H. K. Khalil, "Nonlinear Systems," pp. 245, McMillan, 1992.

[13] Frankel, J. Alvarez, L. Horowitz, R. and P. Li, 1994. Robust Platoon Maneuvers for AVHS. California PATH Technical Note 94-9.

[14] Gerdes, J. C. and J. K. Hedrick, 1996. Vehicle Speed and Spacing Control Via Coordinated Throttle and Brake Actuation. To be presented at the 1996 IFAC Conference, San Francisco, CA.

[15] McMahon, D. H., J. K. Hedrick and S. E. Shladover (1990). Vehicle Modeling and Control for Automated Highway Systems. In: Proc. 1990 ACC, San Diego, CA. pp. 297-303.

[16] Narendran, V. K., 1994. Transition Maneuvers in Intelligent Vehicle Highway Systems. Ph.D. Thesis. University of California at Berkeley.

[17] Swaroop, D. V. A. H. G., 1994. String Stability of Interconnected Systems: An Application to Platooning in Automated Highway Systems. Ph.D. thesis. University of California at Berkeley.

[18] Varaiya, P. and S. Shladover, 1991. Sketch of an IVHS Systems Architecture. University of California, Berkeley: Institute of Transportation Studies. UCB-ITS-PRR-91-3.

[19] Julian Leong, John Tseng, Bret Foreman; "Network Layer Documentation --PATH Wireless Mobile Communications"; Institute of Transportation Stadies, University of California at Berkeley; 1995